TspanC8 tetraspanins regulate ADAM10/Kuzbanian trafficking and promote Notch activation in flies and mammals

Emmanuel Dornier, Franck Coumailleau, Jean-François Ottavi, Julien Moretti, Claude Boucheix, Philippe Mauduit, François Schweisguth, Eric Rubinstein

Published October 22, 2012

TspanC8 tetraspanins regulate ADAM10/Kuzbanian trafficking and promote Notch activation in flies and mammals

Emmanuel Dornier,[1,2] Franck Coumailleau,[3,5] Jean-François Ottavi,[1,2] Julien Moretti,[4,6] Claude Boucheix,[1,2] Philippe Mauduit,[1,2] François Schweisguth,[3,5] and Eric Rubinstein[1,2]

[1]Institut National de la Santé et de la Recherche Médicale (INSERM), U1004, F-94807 Villejuif, France
[2]Université Paris-Sud, Institut André Lwoff, F-94807 Villejuif, France
[3]Département de Biologie du Développement, et [4]Unité de Signalisation Moléculaire et Activation Cellulaire, Institut Pasteur, F-75015 Paris, France
[5]URA 2578, et [6]URA 2582, Centre national de la recherche scientifique (CNRS), F-75015 Paris, France

The metalloprotease ADAM10/Kuzbanian catalyzes the ligand-dependent ectodomain shedding of Notch receptors and activates Notch. Here, we show that the human tetraspanins of the evolutionary conserved TspanC8 subfamily (Tspan5, Tspan10, Tspan14, Tspan15, Tspan17, and Tspan33) directly interact with ADAM10, regulate its exit from the endoplasmic reticulum, and that four of them regulate ADAM10 surface expression levels. In an independent RNAi screen in *Drosophila*, two TspanC8 genes were identified as Notch regulators. Functional analysis of the three *Drosophila* TspanC8 genes (*Tsp3A*, *Tsp86D*, and *Tsp26D*) indicated that these genes act redundantly to promote Notch signaling. During oogenesis, TspanC8 genes were upregulated in border cells and regulated Kuzbanian distribution, Notch activity, and cell migration. Furthermore, the human TspanC8 tetraspanins Tspan5 and Tspan14 positively regulated ligand-induced ADAM10-dependent Notch1 signaling. We conclude that TspanC8 tetraspanins have a conserved function in the regulation of ADAM10 trafficking and activity, thereby positively regulating Notch receptor activation.

Introduction

Cell–cell communication during development and throughout adult life are mediated via secreted and cell surface proteins. Various regulatory mechanisms ensure proper levels of cell–cell interactions and signaling in time and space. One such mechanism involves the regulated processing of cell surface proteins by proteases of the ADAM (a disintegrin and metalloprotease) family. ADAM proteases are type I transmembrane proteins that cleave membrane proteins at sites located close to the membrane, thereby leading to the extracellular release of the ectodomain. This shedding mechanism is essential for cytokine secretion, cell–cell adhesion, and signaling by transmembrane ligands and receptors (Blobel, 2005; Reiss and Saftig, 2009).

ADAM10 is one of the best-characterized members of the ADAM family (Blobel, 2005; Reiss and Saftig, 2009). ADAM10 has several important targets including the amyloid precursor protein (APP) involved in Alzheimer's disease, Fas ligand, several EGF receptor ligands, and Notch receptors. Genetic and biochemical studies have shown that ADAM10, known as Kuzbanian (Kuz) in *Drosophila*, regulates the ligand-dependent processing of Notch at an extracellular site called S2 (Pan and Rubin, 1997; Sotillos et al., 1997; Wen et al., 1997; Brou et al., 2000; Mumm et al., 2000; Hartmann et al., 2002; Lieber et al., 2002; Bozkulak and Weinmaster, 2009; van Tetering et al., 2009). This site is normally protected from ADAM10 cleavage by three Lin12-Notch repeats (LNRs). Upon ligand binding, a ligand-induced conformational change is thought to displace the LNRs, thereby exposing the S2 site to ADAM10 (Gordon et al., 2007; Tiyanont et al., 2011; Meloty-Kapella et al., 2012). S2 cleavage by ADAM10 generates a membrane-tethered form of Notch that is further processed by γ-secretase

E. Dornier, F. Coumailleau, and J.-F. Ottavi contributed equally to this paper.

Correspondence to Eric Rubinstein: eric.rubinstein@inserm.fr; or François Schweisguth: fschweis@pasteur.fr

Abbreviations used in this paper: ADAM, a disintegrin and metalloprotease; Ig, immunoglobulin; LNR, Lin12-Notch repeat; NICD, notch intracellular domain; PDI, protein disulfide isomerise; SOP, sensory organ precursor cell.

The Rockefeller University Press $30.00
J. Cell Biol.
www.jcb.org/cgi/doi/10.1083/jcb.201201133

Published October 22, 2012

at an S3 site located within the transmembrane domain of Notch. S3 cleavage results in the release of the Notch intracellular domain (NICD) that acts in the nucleus to regulate the transcription of Notch target genes (Lecourtois and Schweisguth, 1998; Schroeter et al., 1998; Struhl and Adachi, 1998; De Strooper et al., 1999; Kopan and Ilagan, 2009).

ADAM10 was recently shown to associate with several tetraspanins (Arduise et al., 2008; Xu et al., 2009). Tetraspanins are integral membrane proteins with four transmembrane segments, three short intracellular domains, and a specific fold in the largest of the two extracellular domains. They are expressed in many cell types and have been implicated in various biological processes including cell migration, cell fusion, lymphocyte activation, as well as viral and parasitic infections (Hemler, 2005; Charrin et al., 2009). Tetraspanins are believed to play a role in membrane compartmentalization. This hypothesis is based to a large extent on their unique ability to interact with one another and with non-tetraspanin integral proteins to form a dynamic network of interactions (Hemler, 2005; Charrin et al., 2009). Inside this "tetraspanin web" or "tetraspanin-enriched microdomains," tetraspanins specifically interact with a limited number of partner proteins to form primary complexes. These in turn assemble through tetraspanin–tetraspanin interaction to generate higher order complexes. Primary complexes can be isolated from higher order complexes using detergents such as digitonin, which disrupt tetraspanin–tetraspanin interactions and/or precipitate higher order complexes. Such biochemical approaches have been instrumental to show that the integrins α3β1 and α6β1 form primary complexes with the tetraspanin CD151 and that the Ig domain-containing proteins CD9P-1/EWI-F and EWI-2 are partners of both CD9 and CD81 (Yauch et al., 1998; Serru et al., 1999; Charrin et al., 2001, 2003; Stipp et al., 2001a,b). By contrast, the specific tetraspanins that directly interact with ADAM10 to form primary complexes have not been identified.

In this study, members of a subfamily of tetraspanins that we named TspanC8 were identified as direct and specific partners of ADAM10. In an independent large-scale RNAi screen in *Drosophila*, we uncovered two TspanC8 genes as positive regulators of Notch. Using a combination of in vitro and in vivo assays, we show that TspanC8 tetraspanins regulate the exit of ADAM10/Kuzbanian from the ER, promote its accumulation at the cell surface, and thereby regulate Notch receptor activation in both flies and mammals.

Results

Biochemical identification of TspanC8 tetraspanins as direct partners of ADAM10

Several tetraspanins were previously shown to interact with the mature form of ADAM10 (~68 kD under nonreducing conditions) but not with the immature one (~100 kD, with its prodomain; Arduise et al., 2008; Xu et al., 2009). These coimmunoprecipitation experiments were however performed using a detergent, Brij 97, that preserved tetraspanin–tetraspanin interactions (Fig. 1 A) and therefore did not discriminate between direct and indirect interactions. To reveal specific and direct interactions, coimmunoprecipitations were performed after lysis with digitonin. Using digitonin, ADAM10 did not interact with the classical tetraspanins CD9, CD63, CD81, CD82, and CD151, whereas CD9 still interacted with CD9P-1 (Fig. 1 A and unpublished data). We conclude that the previously reported interactions of tetraspanins with ADAM10 were indirect.

The lack of digitonin-resistant interactions between ADAM10 and classical tetraspanins prompted us to investigate whether less well-characterized tetraspanins could be the direct partners of ADAM10. We initially selected a subset of tetraspanins identified through database mining (Serru et al., 2000). Because no antibodies were available, V5- or GFP-tagged tetraspanins were transiently expressed into PC3 cells that express high levels of ADAM10. Tspan5 (NET-4), but not Tspan1 (NET-1) or Tspan9 (NET-5), was found to coimmunoprecipitate ADAM10 after digitonin lysis (Fig. 1, B and C).

Tspan5 belongs to a subfamily of tetraspanins that are characterized by the presence of eight cysteines in the large extracellular domain (Boucheix and Rubinstein, 2001; Huang et al., 2005). We refer to this family here as TspanC8. This family also includes Tspan10 (occulospanin), Tspan14 (DC-TM4F2), Tspan15 (NET-7), Tspan17, and Tspan33 (penumbra). By contrast with most tetraspanins, TspanC8 family members appeared to be evolutionarily conserved from invertebrates to mammals (Fig. S1). ADAM10 was found to interact in a digitonin-resistant manner with GFP-tagged Tspan14, Tspan15, Tspan33, and, to a lesser extent, with Tspan10 and Tspan17 (Fig. 1 C). By contrast, two GFP-tagged non-TspanC8 tetraspanins, CD9 and Tspan12, did not coimmunoprecipitate ADAM10 (Fig. 1 C). A Tspan5 molecule mutated at all four putative palmitoylation sites still interacted with ADAM10 (Fig. 1 D). Because interactions between tetraspanins rely to a large extent on their palmitoylation (Berditchevski et al., 2002; Charrin et al., 2002; Yang et al., 2002), this result indicated that ADAM10 interacted directly with Tspan5. Direct interactions of ADAM10 with TspanC8 were further suggested by the detection of complexes containing ADAM10 and Tspan5, Tspan14, Tspan15, and Tspan33 after chemical cross-linking (Fig. 1 E). Together, these biochemical data indicate that ADAM10 directly interacts with TspanC8 tetraspanins.

Genetic identification of TspanC8 tetraspanins as Notch regulators

In a parallel approach, two genes of the TspanC8 family, *Tsp3A* and *Tsp86D*, were identified in an RNAi screen for Notch regulators in *Drosophila*. Conditional silencing was achieved using the binary UAS/GAL4 system in combination with the thermosensitive GAL80^{ts} inhibitor. We used the *apterous*-Gal4 driver (*ap-Gal4*) to direct dsRNA expression in imaginal tissues giving rise to the adult dorsal thorax. 11,199 UAS-dsRNA transgenic lines targeting 6,020 genes, i.e., 40% of the fly genome, were screened. This primary screen led to the identification of 272 genes with previously unknown function in sensory organ development (unpublished data). The silencing of *Tsp3A* and *Tsp86D* in imaginal tissues resulted in a weak increase in the number of adult sensory bristles (Figs. S2 and S3), a phenotype

Published October 22, 2012

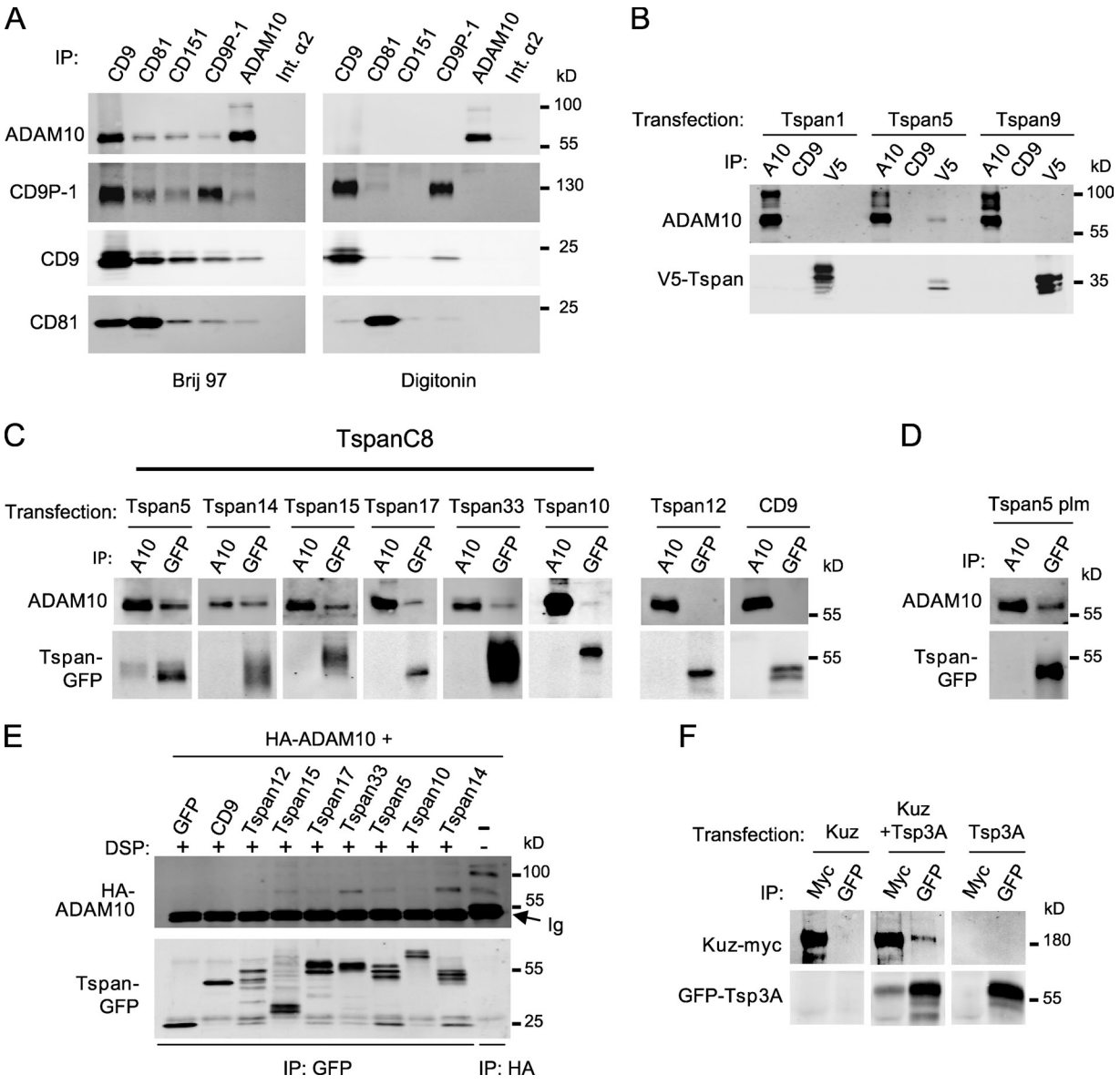

Figure 1. **Several TspanC8 tetraspanins interact with ADAM10 in a digitonin-resistant manner.** (A) HCT116 cells were lysed in the presence of Brij 97 or digitonin before immunoprecipitation with the indicated mAb. The composition of the complexes was analyzed by Western blot. This experiment is representative of several experiments performed with various cell lines. Int.α2: integrin α2. (B) PC3 cells were transiently transfected with V5-tagged Tspan1, Tspan5, or Tspan9 and interaction with ADAM10 was analyzed by coimmunoprecipitation after digitonin lysis and Western blot using mAb to ADAM10 (top) or V5 tag (bottom). A10: ADAM10. (C) PC3 cells were transiently transfected with the indicated GFP-tagged tetraspanins and interaction with ADAM10 was analyzed by coimmunoprecipitation after digitonin lysis and Western blot using mAb to ADAM10 (top) or GFP (bottom). (D) Analysis of ADAM10 interaction with nonpalmitoylatable Tspan5 (Tspan5-plm) after digitonin lysis. (E) HEK 293 cells were transfected with HA-tagged ADAM10 and plasmids encoding either GFP or the indicated GFP-tagged tetraspanins. After cross-linking with DSP, the different tetraspanins were immunoprecipitated using the anti-GFP antibody. The samples were electrophoresed under reducing conditions to break the cross-linker, and the presence of ADAM10 cross-linked to the tetraspanins was detected by Western blot using an anti-HA antibody (top). The efficient immunoprecipitation of the different tetraspanins is controlled by immunoblotting the samples using an anti-GFP antibody (bottom). (F) S2 cells were transiently transfected with plasmids encoding Kuz-myc and GFP-Tsp3A, alone or in combination, and lysed using digitonin. The interaction between Kuz and Tsp3A was analyzed by immunoprecipitation and Western blotting using anti-Myc (Kuz) and anti-GFP (Tsp3A) antibodies. All experiments were performed at least twice.

indicative of reduced Notch activity (Hartenstein and Posakony, 1990). A similar effect was observed in secondary screens using dsRNA and miRNA constructs that did not overlap with the dsRNA transgenes used in the screen (Fig. S3), therefore arguing against off-target effects. Of note, the *Tsp3A* and *Tsp86D* genes were not found in a previous bristle screen for Notch regulators (Mummery-Widmer et al., 2009). Consistent with this, the *Tsp3A* and *Tsp86D* RNAi lines used by Mummery-Widmer et al. (2009) were weaker than those used in our screen (not depicted). Thus, this screen identified Tsp3A and Tsp86D as potential regulators of Notch.

The *Drosophila* TspanC8 family includes a third member, *Tsp26A*, not tested in our screen. Silencing of *Tsp26A* did not affect bristle density (Figs. S2 and S3). The weak (or lack of) RNAi phenotypes seen for the *TspanC8* genes may be due to the partial nature of the silencing effect by dsRNA (Dietzl et al., 2007)

Published October 22, 2012

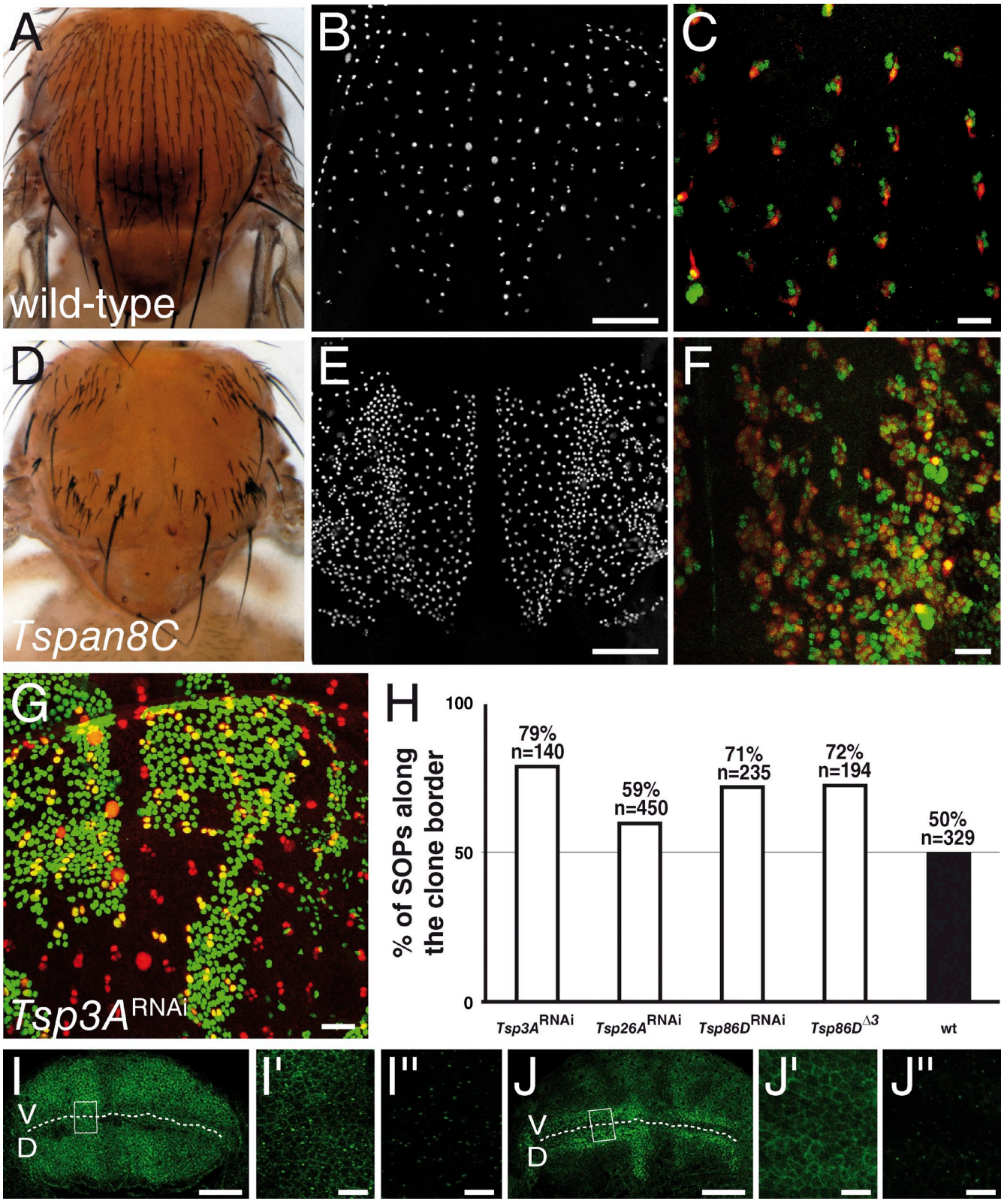

Figure 2. ***Drosophila TspanC8* genes are required for Notch receptor signaling.** (A–F) Wild-type pattern of sensory organs in adult flies (A) and of SOPs in 16 h after puparium formation (APF) pupae (B; positive for nuclear Senseless in white in B and E). At 22 h APF, each sense organ is composed of four cells (C and F; Cut in green). One of these four cells is a neuron (C and F; Elav in red). *TspanC8* flies exhibited a bristle loss phenotype (D) associated with the specification of too many SOPs (E) and the transformation of external cells into internal cells, including neurons (F). *TspanC8* corresponds here to the silencing of *Tsp3A* and *Tsp26A* by ap-GAL4 in a *Tsp86D* heterozygous background (see Table S1 for complete genotype). (G) Clones of cells silenced for *Tsp3A* were marked by nuclear GFP (green) in the notum of developing pupae. Competition for the SOP fate was studied by scoring the genotype (i.e., GFP) of SOPs (Senseless [Sens] in red) along clone borders. (H) Histogram showing the percentage of GFP-positive SOPs along clone borders for various genotypes (*n* is the number of scored SOPs). Control wild-type clones were also studied (wt). For each genotype, the distribution was significantly different

Published October 22, 2012

or to genetic redundancy. To test this possibility, different silencing combinations were tested. All yielded stronger phenotypes than individual silencing (Fig. S3). Strikingly, silencing all three genes or silencing *Tsp3A* and *Tsp26A* in heterozygous *Tsp86D* flies was associated with an increase in the number of sensory organ precursor cells (SOPs; Fig. 2, B and E), a transformation of external sensory cells into internal cells (Fig. 2, C and F), and thereby led to a dramatic bristle loss phenotype (Fig. 2, A and D; and Fig. S3). These three phenotypes are indicative of a strong decrease of Notch activity (Hartenstein and Posakony, 1990). We therefore conclude that these genes act redundantly to regulate the activity of Notch. *Notch*-like phenotypes were also observed in adult wings (Fig. S3) and in ovaries (see following paragraphs). Thus, the *Tsp3A*, *Tsp26A*, and *Tsp86D* genes are required to regulate Notch activity in several developmental contexts.

We next asked whether these *TspanC8* genes act in signal-sending cells to promote ligand activity or in signal-receiving cells to promote receptor activity. To distinguish between these two possibilities, we used a clone border assay that measures the relative ability of cells of different genotypes to compete for the adoption of the SOP fate along mosaic clone borders (Heitzler and Simpson, 1991). In this assay, cells receiving a weaker inhibitory signal are more likely to become SOPs, whereas cells sending a weaker inhibitory signal are more likely to adopt a non-SOP fate. We therefore scored the genotype of SOPs located along the clone borders and found that cells with reduced levels of Tsp3A, Tsp26A, or Tsp86D were more likely to become SOPs (Fig. 2, G and H). This indicated that the *TspanC8* genes act in signal-receiving cells to promote Notch activity. Because the silencing of TspanC8 had no significant effect of the levels and distribution of Notch and Delta (Fig. 2, I–J′′), we wondered whether TspanC8 might regulate Notch indirectly via Kuz, the fly homologue of ADAM10, which also acts in signal-receiving cells to promote the S2 cleavage of Notch (Klein, 2002; Lieber et al., 2002). Consistent with this hypothesis, a Myc-tagged version of Kuz was found to interact in a digitonin-resistant manner with GFP-Tsp3A in *Drosophila* S2 cells (Fig. 1 F). Thus, the molecular interaction between ADAM10/Kuz and TspanC8 is evolutionarily conserved.

Surface accumulation of ADAM10 correlates with high TspanC8 levels

Our identification of TspanC8 tetraspanins as direct partners of ADAM10 and positive regulators of Notch suggested that these proteins may have an essential and conserved function in the regulation of ADAM10/Kuz. To test whether human TspanC8 tetraspanins regulate ADAM10, we screened various carcinoma cell lines for surface expression of ADAM10 and selected three cell lines with high (HCT116 and PC3) and low (HeLa) surface expression of ADAM10 for further analysis (Fig. 3 A). Although HeLa cells expressed slightly less ADAM10 at the mRNA level (Fig. 3 B), we examined whether the observed differences in surface levels reflected differences in subcellular distribution. Consistent with our FACS results, ADAM10 was detected at the surface of nonpermeabilized HCT116 and PC3 cells but was barely detectable at the surface of HeLa cells (Fig. 3 C). However, a perinuclear pool of ADAM10 was detected in HeLa cells upon permeabilization (Fig. 3 C). This intracellular pool colocalized with PDI, an ER marker (Fig. 3 D), suggesting that ADAM10 may be retained in the ER of HeLa cells. Additionally, RT-qPCR analysis showed that HeLa cells expressed low levels of TspanC8, whereas HCT116 and PC3 cells expressed high levels of Tspan14 and Tspan15, respectively (Fig. 3 E). Thus, accumulation of ADAM10 in the ER correlated with low levels of TspanC8, suggesting that TspanC8 tetraspanins may regulate the ER exit of ADAM10.

TspanC8 tetraspanins promote the ER exit and increase cell surface expression of ADAM10

As a first test to determine whether TspanC8 tetraspanins regulate the ER exit of ADAM10, we examined whether the cell surface accumulation of ADAM10 could be restored in HeLa cells by expressing GFP-tagged versions of TspanC8 tetraspanins. Surface levels of ADAM10 were increased up to fivefold upon transient transfection of Tspan5, Tspan14, Tspan15, and Tspan33 (Fig. 4 A), and this was associated with an accumulation of mature ADAM10 (Fig. 4 B). Maximal levels of ADAM10 expression at the cell surface were reached with moderate levels of these tetraspanins. This regulation of ADAM10 appeared to be independent from tetraspanin–tetraspanin interactions because expression of Tspan5-plm, i.e., mutated at predicted palmitoylation sites, similarly increased ADAM10 surface levels. Additionally, this regulation was specific of TspanC8 because transfection of CD9 or Tspan12 had no effect. Conversely, expression of TspanC8 proteins did not affect the expression level of ADAM17 (Fig. S4).

Confocal microscopy analysis shows that expression of Tspan5, Tspan14, Tspan15, or Tspan33 led to the redistribution of ADAM10 from the ER to the cell surface of HeLa cells, where it colocalized with the transfected TspanC8 (Fig. 5 A). To test whether ADAM10 interacts with TspanC8 at the cell surface, cell surface proteins of HeLa cells stably expressing or not Tspan5, Tspan14, or Tspan15 were biotinylated and lysates were subjected to immunoprecipitation using anti-ADAM10 or anti-GFP antibodies (Fig. 4 C). In transfected cells, but not in control cells, anti-GFP precipitated a biotin-labeled protein that co-migrated with ADAM10 (Fig. 4 C) and that was revealed with the anti-ADAM10 mAb in dual-color Western blots. Importantly, in these experiments the level of association of ADAM10 with the transfected TspanC8 was higher than in the

from wild-type (χ^2 test, $P < 0.0001$). (I–J′′) Wing imaginal discs stained for Notch (I–I′′) and Delta (J–J′′) from third instar larvae silenced for *Tsp3A*, *Tsp26A*, and *Tsp86D* using *ap-Gal4* that directs transgene expression in dorsal cells (D; V is ventral; the DV boundary is indicated by a dashed line). I′, I′′, J′, and J′′ (I′ and J′: surface views; I′′ and J′′: −7 µm from the surface) show high magnification views of the area boxed in I and J, respectively. The silencing of the *TspanC8* genes in D cells did not change the levels or distribution of Notch and Delta (compare with control V cells). Bars: (B and E) 100 µm; (C, F, G, I, and J) 25 µm; (I′′ and J′′) 5 µm.

Published October 22, 2012

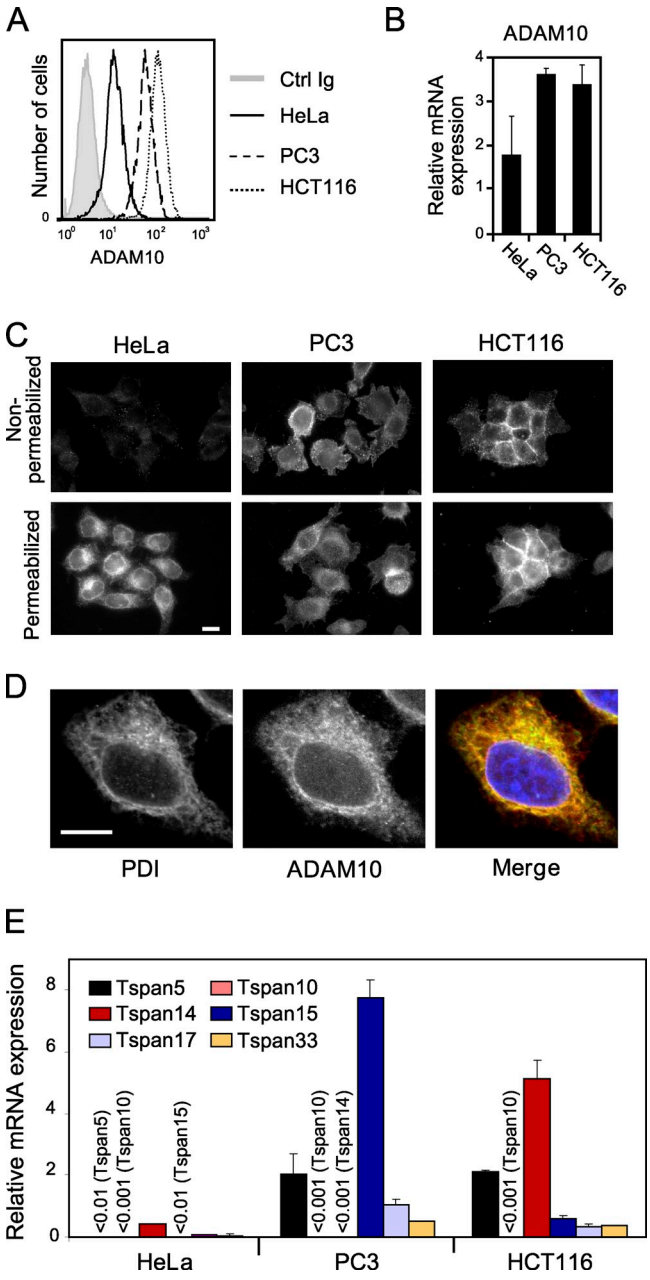

Figure 3. **ADAM10 localization in the ER correlates with low TspanC8 levels.** (A) Flow cytometric analysis of the surface expression of ADAM10 in HeLa, PC3, and HCT116 cells. (B) RT-qPCR analysis of ADAM10 mRNA levels in HeLa, PC3, and HCT116 cells. The figure shows the mean ± SD of three independent experiments performed in triplicate. (C) Surface and intracellular expression of ADAM10 in HeLa, PC3, and HCT116 cells. Cells grown on coverslips were fixed with paraformaldehyde and permeabilized or not with 0.1% Triton X-100 before staining. The acquisition settings were the same for all conditions. This experiment was repeated at least three times. Bar, 10 µm. (D) Confocal microscope analysis of ADAM10 (red) and PDI (green) distribution in HeLa cells permeabilized with 0.1% Triton X-100. This experiment was repeated at least three times. Bar, 10 µm. (E) RT-qPCR analysis of TspanC8 mRNA levels in HeLa, PC3, and HCT116 cells. The figure shows the mean ± SD of three independent experiments performed in triplicate.

experiments shown in Fig. 1. Indeed, similar amounts of ADAM10 were precipitated using anti-GFP and anti-ADAM10 antibodies, suggesting that a large fraction of the ADAM10 pool was in complexes with TspanC8 and reciprocally a fraction of Tspan5, Tspan14, and Tspan15 could also be coimmunoprecipitated with ADAM10 (Fig. 4 C). This stronger association may be due in part to the absence of competition with endogenous TspanC8 in HeLa cells. We therefore conclude that the interaction of ADAM10 with these TspanC8 tetraspanins is quantitatively important and occurs at the cell surface.

In these experiments, Tspan10 and Tspan17 appeared to behave differently than the other TspanC8: Tspan17 had only a moderate effect on ADAM10 surface expression and Tspan10 did not change ADAM10 surface expression or maturation (Fig. 4, A and B). Nevertheless, Tspan10 and Tspan17 appeared to relocalize ADAM10 into a Tspan10- and Tspan17-positive intracellular compartment marked by CD63, a marker of late endosomes (Fig. 5 A and Fig. S4 B), suggesting that Tspan10 and Tspan17 might also promote the ER exit of ADAM10. Together, these results indicated that TspanC8 tetraspanins promote the ER exit and, with the exception of Tspan10 and Tspan17, cell surface accumulation of ADAM10.

We next examined the effect of TspanC8 tetraspanins on the distribution of Kuz in transfected S2 *Drosophila* cells. Expression of GFP-tagged Tsp86D and Tsp3A led to a significant change in the distribution of Myc-tagged Kuz. In control cells, only 4 ± 1% of the Kuz-expressing cells exhibited a clear plasma membrane localization of Kuz. Expression of Tsp86D and Tsp3A increased the percentage of cells with Kuz localizing predominantly at the plasma membrane to 9 ± 3 and 22 ± 2%, respectively (Fig. 5, B–B′′). We therefore propose that the regulation of Kuz/ADAM10 distribution by TspanC8 is conserved across species.

Endogenous TspanC8 tetraspanins are required for the ER exit of ADAM10

We next investigated whether endogenous TspanC8 are required for the surface accumulation of ADAM10. The *Tspan14* and *Tspan15* genes were silenced using siRNAs in HCT116 cells and PC3 cells, respectively. Silencing was strong and specific, as determined by RT-qPCR (Fig. 6 A). In both cases, silencing led to decreased levels of ADAM10 at the cell surface (Fig. 6 B) and to the accumulation of ADAM10 in an intracellular compartment identified as the ER using PDI as a marker (Fig. 6 C). This indicates that endogenous TspanC8 tetraspanins are required to promote the exit of ADAM10 from the ER.

TspanC8 tetraspanins regulate Kuzbanian localization and Notch activity in vivo

To test whether TspanC8 regulate the subcellular distribution of ADAM10/Kuz in vivo, we turned to *Drosophila*. Because no anti-Kuz antibodies are available, we generated a GFP tagged-version of Kuz (Fig. S3). Starting from a 96-kb genomic BAC covering the *kuz* locus (Venken et al., 2006), we used recombineering to generate a Kuz-GFP BAC transgene (Fig. S2; Venken et al., 2009). A single copy of this transgene rescued the lethality of *kuz* mutant flies, indicating that Kuz-GFP is functional and expressed like wild-type Kuz. A very low level of GFP was detected in most larval and imaginal tissues, indicating that Kuz is expressed at low levels, preventing us from studying the distribution of Kuz in these tissues. Previous studies had, however,

Published October 22, 2012

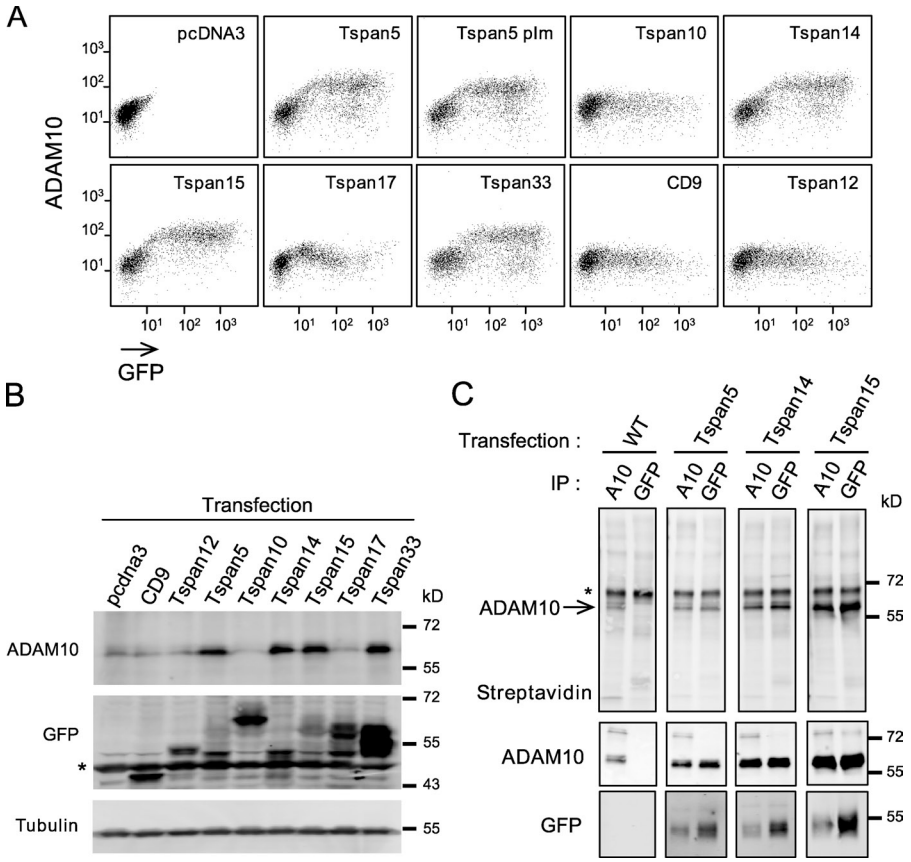

Figure 4. **Expression of TspanC8 in HeLa cells increases the expression of surface and mature ADAM10.** (A) Flow cytometry analysis of the surface expression of ADAM10 in HeLa cells transiently transfected with the indicated GFP-tagged tetraspanins. (B) Western blot analysis of mature ADAM10 and GFP-tagged tetraspanins in transfected HeLa cells. A nonspecific band is indicated by an asterisk. (C) After biotin labeling of surface proteins, HeLa cells stably expressing or not GFP-tagged Tspan5, Tspan14, and Tspan15 were lysed and the interaction of ADAM10 with the transfected tetraspanins was analyzed by coimmunoprecipitation and Western blot. The major 68-kD band revealed by the anti-ADAM10 mAb perfectly overlapped with the band labeled ADAM10 in the top panel. A nonspecific band is indicated by an asterisk. All experiments were performed at least twice with similar outcome.

indicated that the *kuz* gene is expressed at higher levels in a group of migrating cells known as the polar/border cells in ovaries (Wang et al., 2006; Fig. 7 A). Consistent with this, Kuz-GFP was detected in migrating polar/border cells (Fig. 7, D–D′′′). In this context, the activity of *kuz* is required for both Notch signaling and collective cell migration (Wang et al., 2006). Early silencing of the *TspanC8* genes in border cells using the c306 and *slow border* (*slbo*) GAL4 drivers resulted in fewer border cells (Fig. 7 B) and delayed migration (Fig. 7 C). Both phenotypes were also observed upon silencing of *kuz* (Fig. 7, B and C). We therefore used this model system to study the in vivo regulation of Kuz distribution by TspanC8.

First, we observed that Kuz-GFP distributed differently in polar and border cells. Kuz localized into intracellular dots in the two centrally located polar cells, whereas it localized more diffusely at the cell periphery and in the cytoplasm in the 6–8 border cells surrounding the two polar cells. The nature of these Kuz-GFP dots is unclear. In particular, the ER or Golgi markers Sec16, Liquid facet Related, GMAP, and Ofut1 did not mark these dots (not depicted). Despite this, we wondered whether different levels of TspanC8 in polar vs. border cells might account for this difference in distribution. Because transcriptome analysis has suggested that the *Tsp86D* gene is expressed in these migrating cells (Wang et al., 2007), we investigated the expression of *Tsp86D* using a 21-kb genomic BAC encoding a GFP-Tsp86D transgene (Venken et al., 2009). GFP-Tsp86D was expressed at high levels in border cells, whereas polar cells had low levels of GFP-Tsp86D (Fig. 7, E–E′′′). Similarly, we generated a BAC-encoded GFP-Tsp3A and observed that GFP-Tsp3A was also specifically expressed in border cells (Fig. S2). Thus, the intracellular Kuz-GFP dots in polar cells correlated with low levels of Tsp3A and Tsp86D. Furthermore, the silencing of *Tsp3A* and *Tsp26A* in *Tsp86D* heterozygous flies in border cells led to a redistribution of Kuz-GFP into intracellular dots (Fig. 7, F–H; silencing was found to be both efficient and specific in this tissue, as determined using GFP-Tsp3A and GFP-Tsp86D as read-outs: silencing was 80% [Tsp3A] and 97% [Tsp86D] efficient; see Fig. S5). We conclude that TspanC8 tetraspanins regulate the distribution of Kuz in border cells.

A previous study has shown that Kuz regulates Notch in border cells (Wang et al., 2007). To test whether TspanC8 regulates Kuz-dependent Notch signaling in border cells, we used a Notch transcriptional reporter, Gbe-GFP (Housden et al., 2012), expressed in both border and polar cells (Fig. 7, I and I′). The silencing of *Tsp3A* and *Tsp26A* in border cells of *Tsp86D* heterozygous flies led to a significant decrease in Gbe-GFP expression in border but not polar cells (Fig. 7, I–L). Together, our data indicated that TspanC8 tetraspanins regulate the subcellular distribution of Kuz and the activity of Notch in border cells.

TspanC8 tetraspanins positively regulate Notch activity at a pre-γ-secretase step

To test whether human TspanC8 also regulate Notch, HeLa cells were co-cultured with OP9 cells expressing or not the Notch ligand DLL1. A threefold increase in the activity of a CSL-luciferase Notch reporter was induced by DLL1. We next measured Notch activity in HeLa cells stably expressing

Published October 22, 2012

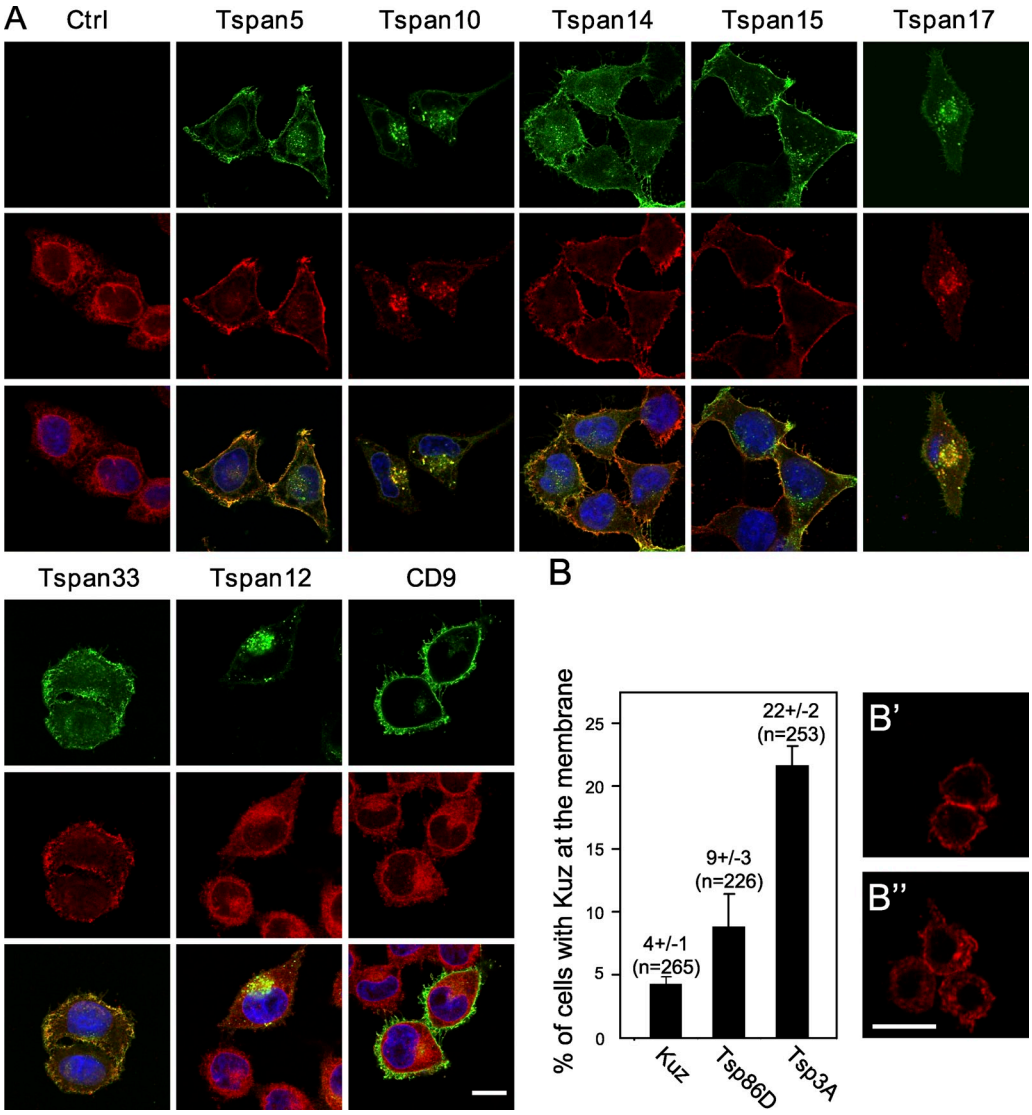

Figure 5. **TspanC8 tetraspanins regulate the subcellular distribution of ADAM10/Kuzbanian in human and *Drosophila* cultured cells.** (A) Confocal microscopy analysis of ADAM10 localization (red) in permeabilized HeLa cells transiently transfected or not with different GFP-tagged tetraspanins (green). Bar, 10 µm. (B) Regulation of the plasma membrane localization of Kuz by Tsp86D and Tsp3A. Transiently transfected S2 cells were scored blind for the localization of Myc-tagged Kuz at the plasma membrane (as in B′) or predominantly in the cytoplasm (as in B′′). Co-transfection of GFP-Tsp86D and GFP-Tsp3A increased the percentage of cells with Kuz at the plasma membrane (B). *n* is the number of cells that were scored. All experiments were performed at least twice with similar outcome.

Tspan5, Tspan14, or Tspan15. HeLa cells expressing Tspan5 and Tspan14, but not Tspan15, showed a 50% increase in OP9-DLL1–induced Notch activity as compared with HeLa cells (Fig. 8 A). These results suggested that the levels of ADAM10 at the cell surface may be limiting for Notch activation in HeLa cells. They also suggested that the Tspan15–ADAM10 interaction may not be sufficient to up-regulate Notch activity.

We next examined the consequence of decreased TspanC8 expression on Notch activity. U2OS cells transduced with human Notch1, i.e., U2OS-N1 (Moretti et al., 2010), were transiently transfected with the CSL-luciferase Notch reporter and co-cultured with OP9 cells expressing or not DLL1. In this assay, luciferase activity increased ∼20-fold in the presence of DLL1 (Fig. 8 B). Activation of Notch1 in U2OS-N1 cells was regulated by ADAM10 because the silencing of ADAM10 decreased OP9-DLL1-induced Notch1 activity (Fig. 8, B and C). Tspan5 and Tspan14 were the major TspanC8 expressed by U2OS cells (unpublished data). Double silencing of these TspanC8 tetraspanins led to an ∼60% reduction in Notch reporter activity, whereas single silencing of Tspan5 or Tspan14 led to an ∼45% and ∼35% reduction, respectively (Fig. 8 B). This effect correlated with a significant decrease in the surface expression levels of ADAM10 (Fig. 8 C), but not of Notch1 (Fig. 8 D). As a control, the silencing of CD81 had no effect. These results indicated that Tspan5 and Tspan14 promote Notch receptor activity in signal-receiving cells.

To determine the step at which TspanC8 tetraspanins act, we measured the effect of Tspan5 and Tspan14 silencing on two constitutively activated versions of Notch1. The first one, NICD,

Published October 22, 2012

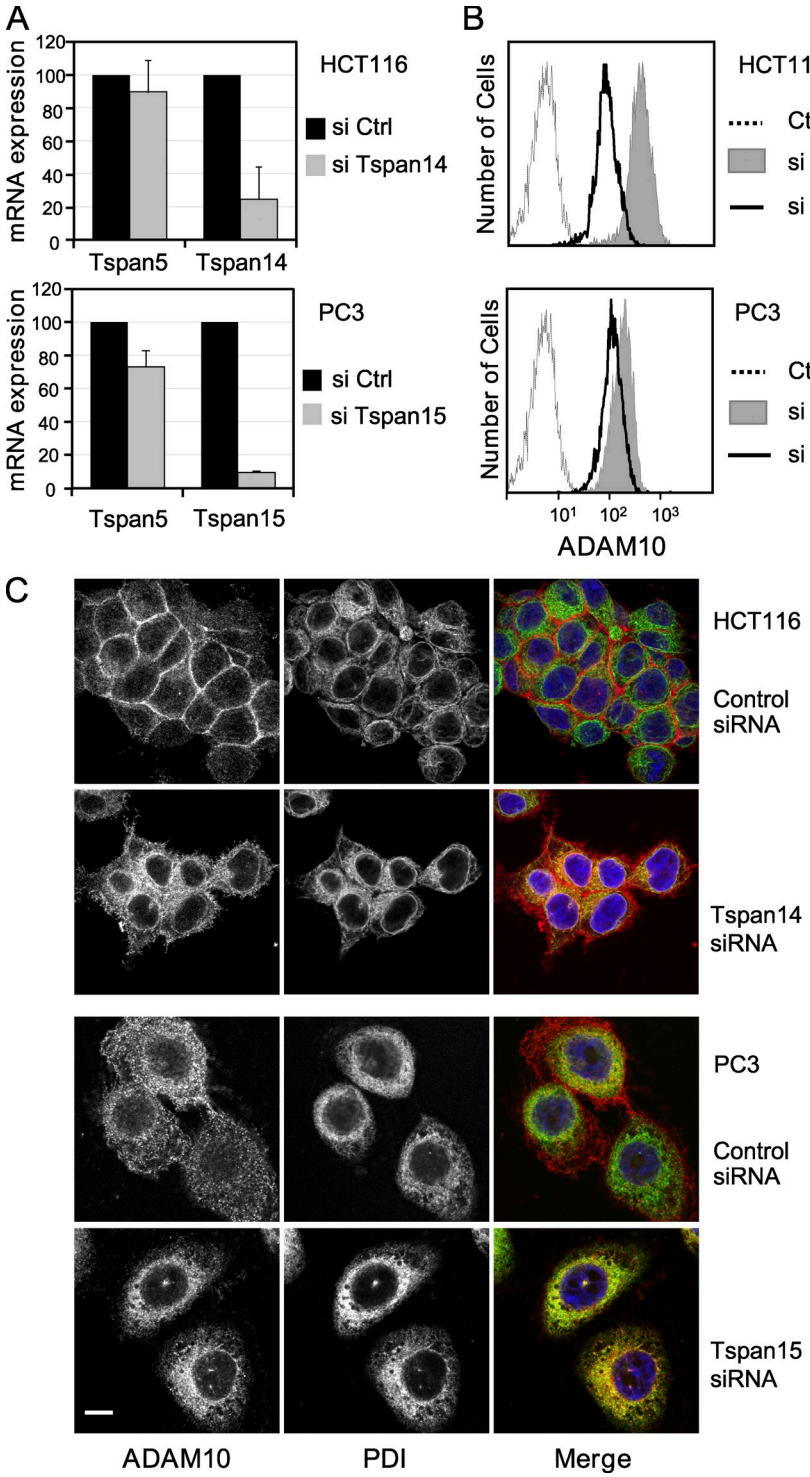

Figure 6. **Endogeneous TspanC8 tetraspanins are required for ADAM10 exit from the ER.** (A) Analysis of Tspan5, Tspan14, or Tspan15 expression using RT-qPCR 24 h after the initiation of Tspan14 or Tspan15 silencing in HCT116 and PC3 cells, respectively. The figure shows the mean ± SD of three independent experiments in triplicate. (B) Flow cytometric analysis of the surface expression of ADAM10 in HCT116 or PC3 cells 2 d after the initiation of Tspan14 or Tspan15 silencing, respectively. (C) Confocal microscope analysis of the distribution of ADAM10 (red) and PDI (green) in Triton X-100 permeabilized HCT116 or PC3 cells after 2 d of silencing with a control siRNA or siRNA targeting Tspan14 (HCT116) or Tspan15 (PC3). Bar, 10 µm. All experiments were performed at least twice with similar outcome.

corresponds to the intracellular domain of Notch1 lacking the PEST domain. The activity of NICD is independent of both ADAM10 and γ-secretase. The second, Notch1-ΔE, contains a short extracellular stub, the transmembrane domain, and the intracellular domain of Notch1 without the PEST domain (Jarriault et al., 1995; Schroeter et al., 1998). The activity of Notch1-ΔE is independent of ADAM10 but dependent on γ-secretase (Mumm et al., 2000). Double silencing of Tspan5 and Tspan14 did not significantly reduce the activities of NICD and Notch1-ΔE (Fig. 8 E). We conclude that TspanC8 tetraspanins regulate Notch receptor activity at a pre–γ-secretase step in signal-receiving cells, which is fully consistent with a regulation of the ADAM10-dependent S2 cleavage of Notch.

Discussion

This study identifies a conserved subfamily of tetraspanins, named here TspanC8, which regulate the localization and activity of ADAM10/Kuz and thereby modulate Notch receptor activation. This conclusion is supported by several key findings:

Published October 22, 2012

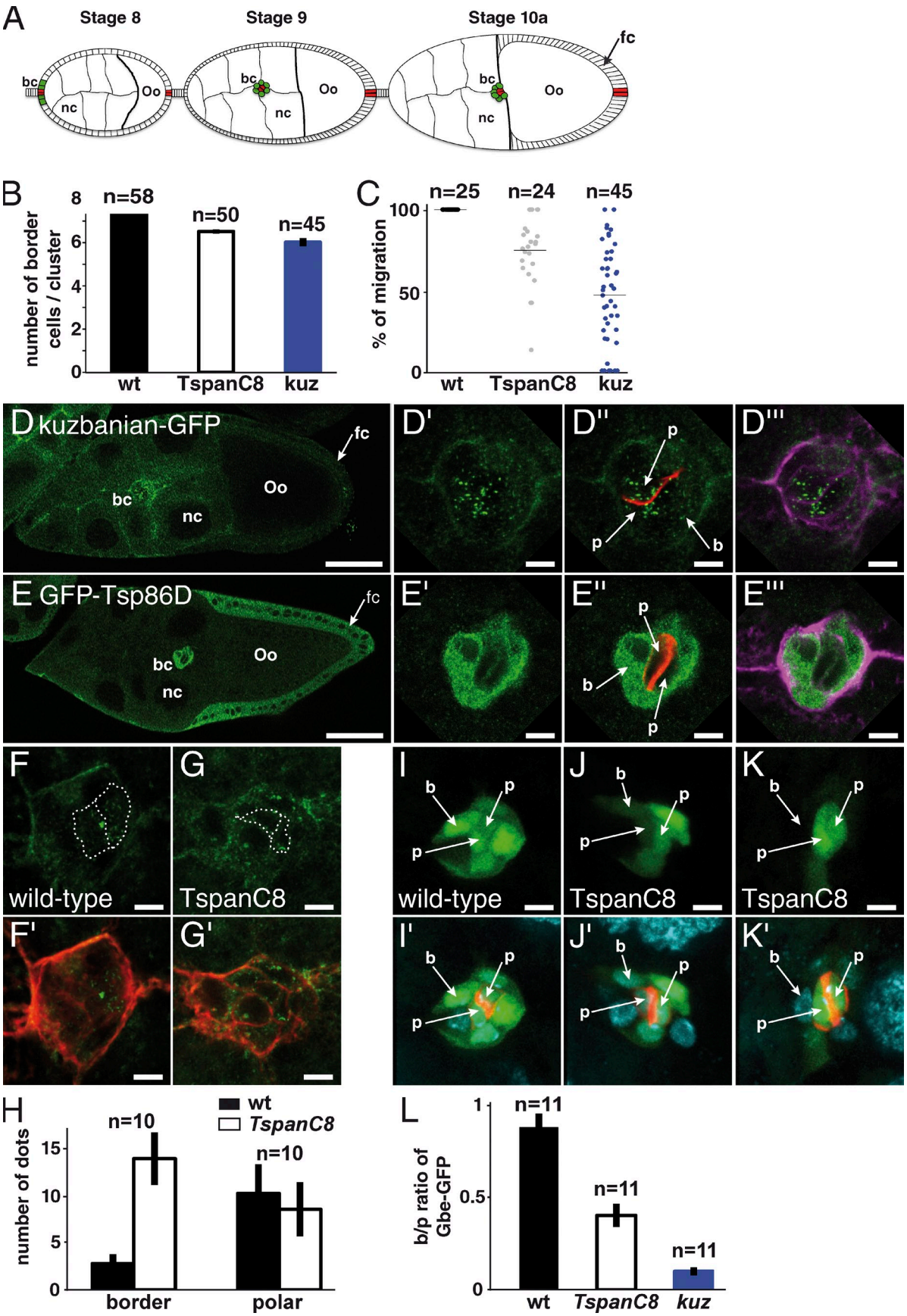

Figure 7. **Regulation of Kuz distribution and Notch signaling in *Drosophila* oocytes.** (A) Schematic representation of egg chambers at stages 8, 9, and 10a (oo, oocyte; nc, nurse cells). Border and polar cells are color coded in green and red, respectively (bc, border cells; fc, follicular cells). (B) In wild-type ovaries, migrating clusters contain 7.8 ± 0.1 border cells. The early silencing of *Tsp3A*, *Tsp26A*, and *Tsp86D* in border cells using *slbo-Gal4 and c306*

Published October 22, 2012

(i) ADAM10 interacts with several TspanC8 tetraspanins in both flies and mammals. (ii) ADAM10 surface expression levels are controlled by TspanC8 both in human cells and in *Drosophila*. (iii) TspanC8 tetraspanins act in signal-receiving cells for the ligand-induced and ADAM10/Kuz-dependent activation of Notch.

This study shows that ADAM10 is a specific and direct partner of all six human TspanC8 tetraspanins. In addition, Tspan5, Tspan14, Tspan15, and Tspan33 increased the expression of ADAM10 at the cell surface and promoted its maturation. A similar finding was recently reported for Tspan15 (Prox et al., 2012). Tspan12 was proposed earlier to interact closely with ADAM10 and to promote its maturation (Xu et al., 2009). However, it did not interact with ADAM10 after digitonin lysis, and did not increase ADAM10 surface expression level and maturation when transfected in HeLa cells. These data, together with the observation that the interaction of ADAM10 with Tspan12 required its palmitoylation (Xu et al., 2009), strongly suggest that Tspan12 interacts only indirectly with ADAM10. Additionally, Tspan10 and Tspan17 behaved differently from other TspanC8 tetraspanins because their expression induced the intracellular redistribution of ADAM10 in HeLa cells. We therefore suggest that different TspanC8 may provide ADAM10 with different trafficking properties.

How do Tspan5, Tspan14, Tspan15, and Tspan33 regulate the expression level of mature ADAM10? A possibility, consistent with their interaction at the cell surface, is that these tetraspanins act by stabilizing ADAM10 at the plasma membrane. This increase in mature ADAM10 expression is also probably, to some extent, a direct consequence of the ability of TspanC8 to mediate the ER exit of ADAM10. ADAM10 is retained in the ER through a mechanism involving an arginine-based motif (Marcello et al., 2010) that may function as an ER retention signal. Such arginine-based motifs are often found in subunits of multi-molecular complexes and are masked upon complex assembly, thereby allowing ER exit of the properly assembled complexes (Michelsen et al., 2005). We therefore suggest that TspanC8 tetraspanins allow for the ER exit of ADAM10 by masking its arginine-based motif. A role of tetraspanins in the ER exit of their molecular partner is probably not restricted to TspanC8 tetraspanins, as suggested by the differential expression and/or maturation of CD19 and EWI-2 in the presence or not of their partner tetraspanins (Shoham et al., 2003; Stipp et al., 2003; He et al., 2009). Although an ER retention motif has yet to be defined in EWI-2 or CD19, both proteins contain a putative arginine-based motif (unpublished data).

Our results indicating that several human TspanC8 family members have a similar molecular activity on the regulation of ADAM10 are consistent with our RNAi analysis showing that the fly *TspanC8* genes act redundantly to regulate Notch. However, one limitation of this RNAi approach is that silencing is often incomplete (Dietzl et al., 2007), so that residual activity might hinder some aspects of the null mutant phenotype. Despite this limitation, our data clearly established that TspanC8 tetraspanins play an essential role for proper Notch activity in various developmental settings. Kuz is likely to be the main target of TspanC8 in *Drosophila*. First, our clone border analysis indicated that the activity of TspanC8, like that of Kuz, is required in signal-receiving cells. Second, the distribution of Kuz, but not those of Notch and Delta, appeared to be regulated by TspanC8. Third, Kuz appeared to interact with Tsp3A (interaction with Tsp26A and Tsp86D was not tested). Our data further indicated that the relevant target of Kuz is Notch, rather than its ligand Delta. Although Kuz can down-regulate Delta (Qi et al., 1999; Mishra-Gorur et al., 2002), hence potentially interfering with its cis-inhibitory activity (del Álamo et al., 2011), Delta levels remained unchanged upon TspanC8 silencing. Moreover, human Tspan5 and Tspan14 positively regulated ligand-induced ADAM10-dependent Notch1 signaling at a pre-γ-secretase step in an assay where ligands act in trans. Together, our data support the view that TspanC8 tetraspanins regulate Notch activity via the regulation of the ADAM10/Kuz-mediated S2 cleavage. Also consistent with this view are the synergistic interactions observed between the *C. elegans* TspanC8 family member *tsp-12* and *sup-17*, the ADAM10 orthologue. *tsp-12* was identified as a suppressor of a mutation causing constitutive or elevated activity of GLP-1, one of two Notch-like receptors in *C. elegans* (Dunn et al., 2010). However, Tsp-12 was proposed to act by facilitating the S3 (rather than the S2) cleavage of GLP-1. This interpretation relied to a large extent on the observation that Tspan33 silencing in HeLa cells reduced the activity of Notch1-ΔE but had no effect on NICD. Whether Tspan33 regulates γ-secretase activity indirectly via the

led to a reduced number of border cells (6.5 ± 0.1), similarly to *kuz* silencing (6.0 ± 0.2). (C) Plots showing the raw distribution of the relative distance covered by individual clusters along the migratory path at stage 10a. In wild-type ovaries, all clusters (n = 25) have completed their migration (distance covered: 100%). The silencing of *kuz* and *TspanC8* resulted in a significant migration delay because clusters covered only 45 ± 26% and 75 ± 16% of the total distance, respectively, at stage 10a. (D–E‴) Distribution of Kuz-GFP and GFP-Tsp86D (anti-GFP in green) in stage 9 egg chambers. Kuz and Tsp86D were expressed in migrating somatic cells consisting of two central polar cells (p; marked by Fas3, red in D″ and E″) surrounded by 6–8 border cells (b; outlined by actin, violet in D‴ and E‴). Kuz-GFP mostly localized into dots in polar cells but was diffusely distributed in border cells (D′–D‴). Tsp86D was expressed in border cells (E′–E‴) and in the somatic follicular cells (fc) around the oocyte. (F–G′) The silencing of *TspanC8* in border cells, i.e., the triple *Tsp3A*, *Tsp26A*, and *Tsp86D* RNAi using *slbo-Gal4*, led to the redistribution of Kuz-GFP (green) into dots in border cells (G and G′; compare with control heterozygous Kuz-GFP in F and F′; actin, red). (H) Quantification of the Kuz-GFP dots in border and polar cells. The silencing of *TspanC8* in border cells specifically increased the number of Kuz-GFP dots in these cells (14 ± 3 relative to 3 ± 1 in controls). No significant effect was seen in polar cells (9 ± 3 relative to 10 ± 3 in controls). (I–K′) Notch reporter gene activity (green; Fas3, red; DAPI, blue) was detected in border (b) and polar (p) cells (I and I′). *TspanC8* silencing in border cells resulted in decreased Notch reporter activity. This effect varied from medium (J and J′) to strong (K and K′). (L) Ratiometric analysis of the GFP signal from the Notch reporter Gbe-GFP in migrating border cells relative to polar cells. The silencing of *TspanC8* and *kuz* genes (as in I–K′) led to reduced border/polar ratios in GFP intensity (0.40 ± 0.06 and 0.10 ± 0.02, respectively; wild-type was 0.88 ± 0.07). Bars: (D and E) 40 µm; (all other panels) 5 µm.

Published October 22, 2012

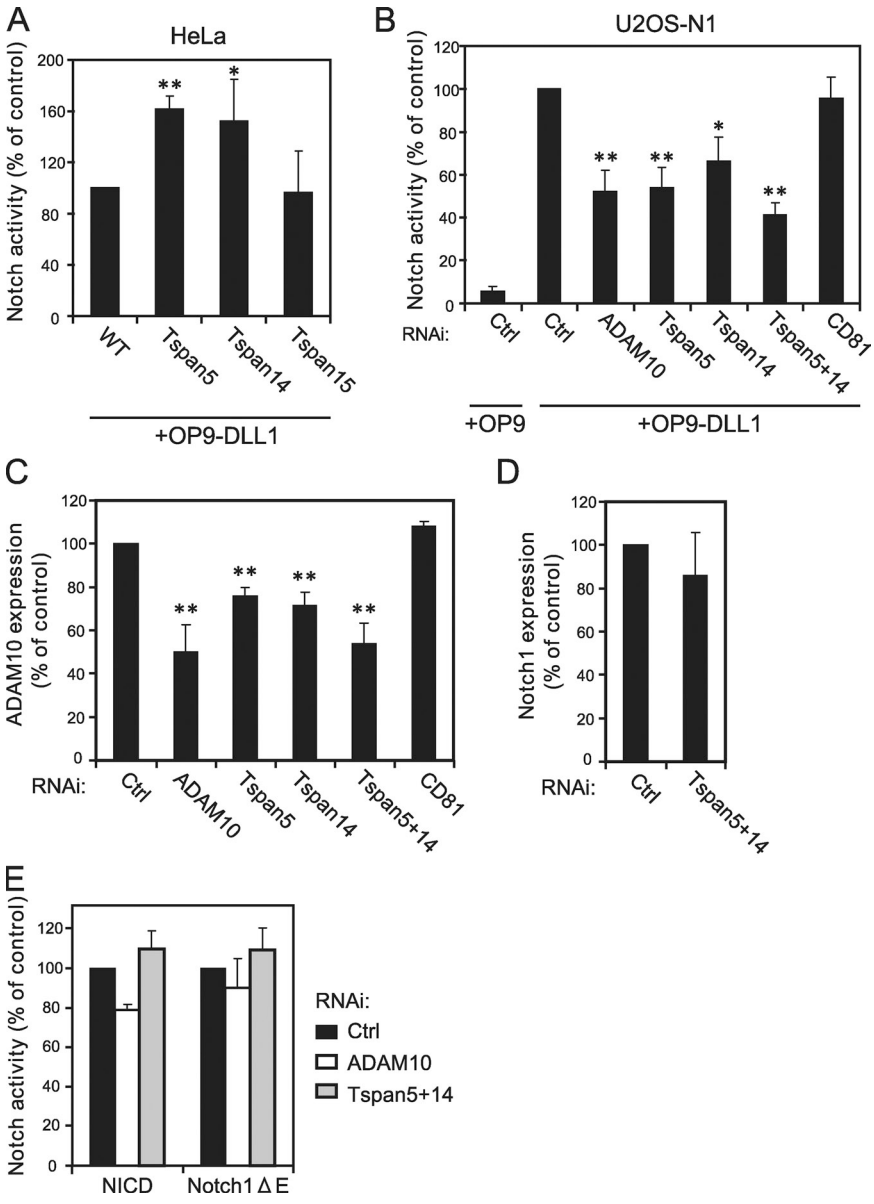

Figure 8. **Tspan5 and Tspan14 regulate ligand-induced Notch activation.** (A) Notch activity measured using a CSL reporter luciferase assay, of HeLa cells stably expressing or not Tspan5, Tspan14, or Tspan15. Notch was activated by incubation with OP9-DLL1 cells. The figure shows the mean ± SD of four independent experiments in duplicate. (B) U2OS-N1 cells were treated with the indicated siRNA before analysis of Notch activity produced by incubation with OP9 or OP9-DLL1 cells. The figure shows the mean ± SD of three independent experiments performed in duplicate. (C) Flow cytometric analysis of the surface expression of ADAM10 in U2OS-N1 cells treated with the indicated siRNA. The figure shows the mean ± SD of three independent experiments. (D) Flow cytometric analysis of the surface expression of Notch1 in U2OS-N1 cells treated with a control siRNA or siRNa directed to both Tspan5 and Tspan14. The figure shows the mean ± SD of three independent experiments. (E) U2OS-N1 cells were treated with the indicated siRNA and transfected with NICD and Notch1-ΔE constructs. Notch activity was determined using the luciferase assay. The figure shows the mean ± SD of three independent experiments performed in duplicate. **, $P < 0.01$; *, $P < 0.05$ as compared with control cells.

non-TspanC8 tetraspanins that were found associated with γ-secretase (Wakabayashi et al., 2009) remains to be determined. Whatever the molecular basis, this result contrasts with our data showing that the silencing of both Tspan5 and Tspan14 significantly decreased ligand-mediated Notch activation but had no effect on the activity of Notch1-ΔE. Unfortunately, we could not investigate the role of Tspan33 in the S2 and S3 processing of Notch1 because none of the cell lines tested here, including HeLa, expressed Tspan33 at a significant level.

In conclusion, this study establishes that the trafficking and activity of ADAM10 are regulated by tetraspanins of the TspanC8 family and that this regulation has important consequences in terms of Notch signaling. Further work should determine why ADAM10 associates with so many tetraspanin partners. We hypothesize that these different tetraspanins may provide ADAM10 with different trafficking properties (Tspan10 and Tspan17) or differentially restrict the range of its substrates, as suggested by the lack of effect of Tspan15 transfection on Notch activity in HeLa cells. This new link has potential implications for the interpretation of phenotypes associated with defective TspanC8 activity, and further work should determine whether the defect in erythropoiesis of *Tspan33* (penumbra) mutant mice is linked to a defect of ADAM10 and/or Notch function (Heikens et al., 2007). Finally, because ADAM10 is a promising therapeutic target in various pathologies (Saftig and Reiss, 2011) and because mouse TspanC8 genes display tissue-specific expression (Wu et al., 2009), it might be envisaged to inhibit ADAM10 activity in a tissue-specific manner by interfering with the activity of specific TspanC8.

Materials and methods

Reagents for in vitro studies

The mouse mAb anti–human ADAM10 11G2 was described in Arduise et al. (2008); the mouse mAb anti–human Notch1 and anti–human ADAM17 were from R&D Systems and the anti–human PDI from Abcam. The anti-tag

Published October 22, 2012

antibodies used in this study were anti-GFP (a mouse mAb coktail from Roche and a rabbit polyclonal from Santa Cruz Biotechnology, Inc.), anti-HA (HA11 mouse mAb from Covance), and anti-V5 (a mouse mAb and a rabbit polyclonal from Sigma-Aldrich). The following siRNAs were obtained from Invitrogen and Eurogentec: control siRNA: Stealth RNAi Negative Control Medium GC; Tspan5: AUGUCAUCCCGAUAUGCUCUGAUGU; Tspan14: CGCCAUCUCGCUGUUGCAGAUAUUU; Tspan15: ACAACCUGUACCUUCUCCAAGCAUU; and CD81: GCACCAAGUGCAUCAAGUA-dTdT.

All V5- or GFP-tagged tetraspanin cDNA were of human origin. Coding regions were amplified by PCR from previously described plasmids (Tspan1, Tspan5, Tspan9, Tspan12, and Tspan15; Serru et al., 2000), from plasmids obtained from Open Biosystems (Tspan10 and Tspan33), or from a reverse-transcription performed on HCT116 RNA (Tspan14). PCR products were subcloned into pEGFP-N1, pEGFP-N3, or pcDNA 3.1 Directional TOPO vectors. hTspan17 and Tspan5-plm were synthesized by Eurogentec. The mouse myc-tagged Notch1 constructs ΔE and NICD (in the pCS2+MT vector) and the HA-tagged bovine ADAM10 (in pCDNA3) were described previously (Jarriault et al., 1995; Lammich et al., 1999).

The cell lines HeLa (cervical carcinoma), HCT116 (colon carcinoma), PC3 (prostate carcinoma), and HEK293 (human embryonic kidney) were cultured in DME containing 10% FCS and antibiotics. Cells were transfected with either Fugene 6 (Promega) or Lipofectamine 2000 (Invitrogen) according to the manufacturers' instructions. OP9 cells expressing the human Notch ligand DLL-1 (OP9-DLL-1) and the human osteosarcoma cell line U2OS expressing human Notch1 (U2OS-N1) were obtained by infection with retroviruses carrying the DLL1 cDNA cloned in the MSCV-IRES-GFP vector and a human Notch1 cDNA cloned in the pBabe puro vector, respectively. These two cell lines are described in Moretti et al. (2010) and Six et al. (2004). S2 cells were transfected using FugeneHD (Promega) following the manufacturer's instructions.

S2 cells were transfected with pMT-Gal4 (obtained from the Drosophila Genomics Resource Center), pUAS-GFP-Tsp3A, and Myc-tagged Kuz using FugeneHD (Promega) according to the manufacturer's instructions. Expression of GFP-Tsp3A in S2 cells was monitored for 16–20 h after induction with 500 µm of $CuSO_4$, and cells were immunostained following standard procedures. The *Tsp3A* ORF was PCR amplified from cDNAs prepared from wild-type total embryonic RNAs and fused in-frame downstream of EGFP with a YSDLR linker, sequenced and cloned into a pUASt vector to generate pUAS-GFP-Tsp3A. Myc-tagged Kuz corresponds to the *kuz* ORF with a 6x Myc epitope tag at its C terminus under an actin promoter (Lieber et al., 2002).

Flow cytometry analysis

Cells were detached, washed twice in complete DME and incubated for 30 min at 4°C with 10 µg/ml primary antibody. After three washings, the cells were incubated for 30 min at 4°C with a fluorochrome-conjugated $F(ab')_2$ goat anti–mouse antibody (FITC or PE for single color staining of nontransfected cells; APC for staining of cells transfected with GFP constructs). The cells were analyzed using a FACSCalibur or an Accuri C6 flow-cytometer (BD), using appropriate compensations. Cells were detached using a nonenzymatic solution (PAA), except for the analysis of Notch1 expression for which they were detached in 15 mM sodium citrate, 0.135 mM potassium chloride.

Analysis of Notch activity in mammalian cell lines

This analysis was performed as described previously (Moretti et al., 2010): U2OS-N1 or HeLa cells were seeded at the concentration of 25,000 cells/cm^2. Silencing was performed at this step using Interferin (PolyPlus Transfection) and 3 nM siRNA according to the manufacturer's reverse procedure. Cells were transfected 24 h later with the CSL reporter and Renilla control plasmids using FuGENE 6 (Promega). 24 h later, cells were co-cultured with OP9 or OP9-DLL1 at 35,000 cells/cm^2. The activities of firefly and Renilla luciferases were determined using a Dual luciferase reporter assay (Promega) according to the manufacturer's instructions. Statistical analysis was performed using one-way ANOVA followed by Tukey's multiple comparison test.

Immunoprecipitation, chemical cross-linking, and biotin labeling of surface proteins

Biotin labeling of surface proteins and immunoprecipitations were performed as described previously (Charrin et al., 2001; Arduise et al., 2008). In brief, biotin-labeled or nonlabeled cells were lysed in a lysis buffer containing 30 mM Tris, pH 7.4, 150 mM NaCl, protease inhibitors, and 1% detergent (Brij 97 or digitonin). After 30 min incubation at 4°C, the insoluble material was removed by centrifugation at 10,000 *g* and the cell lysate was precleared by addition of heat-inactivated goat serum and protein G–Sepharose beads (GE Healthcare). Proteins were then immunoprecipitated by adding 1 µg mAb and 10 µl protein G–Sepharose beads to 200–400 µl of the lysate. The immunoprecipitated proteins were separated by SDS-PAGE under nonreducing conditions and transferred to a PVDF membrane (GE Healthcare). Western blotting on immunoprecipitates was performed using either Alexa Fluor 680–labeled 11G2 mAb or a combination of rabbit anti-GFP antibody and a secondary reagent labeled with IRDye800. Acquisition was performed using the Odyssey Infrared Imaging System (LI-COR Biosciences).

For cross-linking, HEK 293 cells were transiently transfected with HA-ADAM10 and various GFP-tagged tetraspanins. 48 h after transfection, the cells were treated with 1 mM dithiobis[succinimidyl propionate] (DSP) for 30 min at 4°C, and lysed in lysis buffer supplemented with 1% Triton X-100 and 0.2% SDS before immunoprecipitation.

Quantitative RT-PCR

Total RNA fraction was isolated from 5×10^6 cells of different cell lines using the SV Total RNA Isolation System including an on-column DNase digest (Promega) according to the manufacturer's instructions. Subsequently, cDNA was synthesized from 5 µg of total RNA from each sample using 200 U of SuperScript III Reverse transcription (Invitrogen) primed with random hexamer (Promega). Quantitative real-time polymerase chain (QPCR) reactions were then performed in a final volume of 25 µl containing 2x Brillant II SYBR Green QPCR Master Mix from Agilent Technologies, 0.4 µM each forward and reverse primers and 62.5 µg of cDNA. Quantification was performed with the Mx3005P QPCR Systems and MxPro software from Agilent Technologies. For each cDNA sample, triplicates were analyzed and data normalized to rpl38 expression according to the ΔCt method. Most oligonucleotides were designed by primer bank (Spandidos et al., 2010). Tspan5: ACAAGGGTCCTGAAGTCAGTT and TGATGGAAGAGATGTTGGACAGA; Tspan10: CTGCGTCAAGTATCTGATCTTCC and AAGCCACGTAACAGGCAGG; Tspan14: GGCTCTGCGGGAGAATATCTG and GCACTGGTTAGCTTTCTGAAGG; Tspan15: ACTTCCTGAACGACAACATTCG and CGCCACAGCACTTGAACTTTT; Tspan17: CTGCTGCGGGAAATACTTCCT and GATGTTCGAGAGAACGCCCTT; Tspan33: CTACGCTCGGCTAATGAAGCA and TGAGCAGGAACATGAGGACAC; ADAM10: AAACACCAGCGTGCCAAAAG and CCCTCTTCATTCGTAGGTTGAAA.

Immunostainings and microscopy

Human cells were grown in complete medium for 24 h on coverslips. For comparison of surface and internal distribution of ADAM10, the cells were fixed for 30 min with 4% paraformaldehyde at room temperature, blocked for 15 min with 50 mM NH_4Cl in PBS, and permeabilized or not with 0.1% Triton X-100 at 4°C for 2 min. The cells were then incubated for 1 h with 10 µg/ml of the anti-ADAM10 mAb 11G2 (IgG1) in complete DME at room temperature. For double labeling the cells were coincubated with an antibody to the ER marker PDI (IgG2a). Primary antibodies were revealed with Alexa Fluor 488– and Alexa Fluor 568–labeled goat anti–mouse IgG1 and IgG2a antibodies. The cells were mounted in Mowiol 4-88 (81381; Sigma-Aldrich) supplemented with DABCO (D2522; Sigma-Aldrich) and DAPI and examined at room temperature either with a DMR fluorescence microscope (Leica) equipped with a CoolSnap HQ2 camera (Photometrics) controlled by MetaMorph (Molecular devices), or an SP5 confocal microscope (Leica) using 63x oil objectives (NA 1.32 and 1.40, respectively).

Drosophila imaginal discs, nota, and egg chambers were dissected from staged larvae, pupae, and female flies, respectively, and stained using standard techniques. Primary antibodies used in *Drosophila* were: goat anti-GFP (1:500; ab5450 from Abcam), guinea pig anti-Senseless (1:3,000; a gift from H. Bellen, HHMI, Baylor College of Medicine, Houston, TX; Nolo et al., 2000), rabbit anti-dGMAP (1:1,000; a gift of P. Therond, CNRS, Nice, France; Friggi-Grelin et al., 2006), rabbit anti-dSec16 (1:200; a gift of C. Rabouille, Hubrecht Institute, Utrecht, Netherlands; Ivan et al., 2008), guinea pig anti-Ofut1 (1:1,000; a gift of K. Irvine, HHMI Rutgers University, Piscataway, NJ; Okajima et al., 2005), guinea pig anti-Lqfr (1:100; a gift of J. Fischer, University of Texas, Austin, TX; Lee et al., 2009), rat anti-Su(H) (1:2,000; Gho et al., 1996), mouse anti-NECD (C458.2H, 1:100; Developmental Studies Hybridoma Bank [DSHB]), mouse anti-Delta (C594.9B, 1:100; DSHB), mouse anti-Fas3 7G10 mAb (1:100; DSHB), mouse anti-Cut 2B10 mAb (1:500; DSHB), rat anti-Elav 7E8A10 mAb (1:100; DSHB), and rabbit anti-Myc (1:500; EMD Millipore). Secondary antibodies were from Jackson ImmunoResearch Laboratories and coupled to Cy2, Cy3, and Cy5. Atto 647N-Phalloidin (65906; Sigma-Aldrich) was used at 0.1 µM to stain F-actin. Nota and egg chambers were mounted in Mowiol 4-88 (81381; Sigma-Aldrich) containing 2.5% of DABCO (D2522; Sigma-Aldrich). Images were acquired using an

Published October 22, 2012

SPE confocal microscope (Leica) using 20x (HCX PL APO CS, NA 0.6), 40x (HCX PL APO CS, NA 1.4), and 63x (HCX PL APO CS, N.A. 1.3) objectives. Adult flies were imaged using a Discovery V20 stereomicroscope (Carl Zeiss) using a 1.0x objective (PlanApo S FWD 60 mm).

Images were processed using ImageJ (National Institutes of Health) and Adobe Photoshop software. Categorization of the plasma membrane vs. cytoplasmic accumulation of Kuz-Myc in S2 cells, using the cell outline and the nucleus as landmarks, was performed blind after randomization of the images. To quantify the Gbe-GFP signal at stage 9–10a, the GFP signal was measured in each polar and border cell on a single confocal section running across the nucleus using ImageJ. Values were corrected by subtracting the background signal measured outside the egg chamber. For each egg chamber, mean values were calculated for the 2 polar and for the 6–10 border cells. These two mean values defined a border/polar ratio. The extent of border cell migration was measured as the percentage of migration within individual stage 10a egg chambers. To characterize the distribution of Kuz-GFP in border and polar cells, 512 × 512 images acquired at 63x (zoom 6) were thresholded and the number of "objects" >8 pixels in size were counted.

Drosophila transgenes and mutations

The *kuz*$^{[k01405]}$ (Sotillos et al., 1997), *kuz*$^{[e29-4]}$ (Pan and Rubin, 1997), and the transgenic conditional RNAi flies have been described previously: UAS-dsRNA*Tsp3A* (10742R-2 and 10742R-3; from R. Ueda, http://www.shigen.nig.ac.jp/fly/nigfly/index.jsp); 10138 and 10140 from the Vienna Drosophila Rnai Center [VDRC] (Dietzl et al., 2007); UAS-dsRNA*Tsp86D* (4591R-1 and 4591R-2 from R. Ueda; 102046, 42642, and 42643 from the VDRC); UAS-dsRNA*Tsp26A* (101473 from the VDRC); and UAS-dsRNA*kuz* (103555 from the VDRC). Conditional silencing was achieved using the binary UAS/GAL4 system in combination with the thermo-sensitive GAL80^{ts} inhibitor. We used the *apterous*-Gal4 driver (*ap-Gal4*) to direct dsRNA expression in imaginal tissues giving rise to the adult dorsal thorax, and a combination of *c306* and *slow border* (*slbo*) Gal4 drivers to direct dsRNA expression in border cells. (Manseau et al., 1997; Rørth et al., 1998).

The *Tsp86D*$^{\Delta 3}$ deficiency that removes the *Tsp86D* gene was generated by Flp-FRT as described in Parks et al. (2004). The 5′- and 3′-flanking elements were the P{XP}Fdh^{d04974} and PBac{RB}*CG6574*^{e00293}, respectively. This 9,442-nt deletion removes the *CG6574*, *SelR*, *Tsp86D*, and *Fdh* genes (Fig. S3). Breakpoints were confirmed by PCR (primers sequences available upon request).

The *kuz-GFP*, *GFP-Tsp3A*, and *GFP-Tsp86D* transgenes were generated by BAC recombineering in *E. coli* SW102 as described at http://web.ncifcrf.gov/research/brb/recombineeringInformation.aspx (Venken et al., 2006). The starting BACs were generated by Venken et al. (2009) and were obtained from BACPAC (http://bacpac.chori.org).

The CH321-04I18 BAC covering the *kuz* locus from −6,996 nt 5′ to the transcription start site to 3,040 nt downstream of the 3′UTR was used. PCR products corresponding to the 5′ and 3′ homology arms were produced using the following primers: Kuz5F: GACAGCAGCAAATGCAACAGCA; Kuz5Rgfp: CTTGCTCACCATTAGGACTGCATAAACGATATTTCGGCG; Kuz3Fgfp: CTGTACAAGTAAGAGCGGAACCATCACATT; and Kuz3R: CACATACTTGGTTAGTGCAGT.

The GFP cassette included an AVL linker. It was amplified using the following primers: KuzGfpF: AATATCGTTTATGCAGTCCTAATGGTGAGCAAGGGCGAG; KuzGfpR: ATGGTTCCGCTCTTACTTGTACAGCTCGTC. The BAC CH322-135L04 extended 8,002 nt 5′ to the transcription start site and 8,378 nt downstream of the 3′UTR of the *Tsp3A* gene. The 5′ and 3′ homology arms and the GFP cassette were PCR amplified using the following primers: 5′FN_3A: CTCAAAGGTCAGTGCCGAAACGA; 5′T3A_GFP_R: CTTGCTCACCATCCTCGCCGTTTATCTGTA; 3′T3A_GFP_F: TAAACGGCGAGGATGGTGAGCAAGGGCGAG; 3′NR_3A: CAGACGATGGCTGTTGGCGCAGACA; 5′T3A_GFP_F: TACAAGCTGCCAGCAGGAATGAGCAACTACCGATAT; and 3′T3A_GFP_R: CTCATTCCTGCTGGCAGCTTGTACAGCTCGTCCAT. The BAC CH322-137B04 extended 8,496 nt 5′ to the transcription start site and 8,733 nt downstream of the 3′UTR of the *Tsp86D*. The 5′ and 3′ homology arms and the GFP cassette were PCR amplified using the following primers: 5′FN_86D: GTCGCAATGTTACGCAGCGGTGGA; 5′T86D_GFP_R: CTTGCTCACCATGGCCACGCGAATGTGCAA; 3′T86D_GFP_F: TACAAGCTGCCAGCAGGAATGAGCAATCACAGATAC; 3′NR_86D: TGCAAGTCGGAGTCGTCACGGTACGA; 5′T86D_GFP_F: ATTCGCGTGGCCATGGTGAGCAAGGGCGAG; and 3′T86D_GFP_R: CTCATTCCTGCTGGCAGCTTGTACAGCTCGTCCAT.

Constructs were verified by sequencing of the recombined regions before phiC31-mediated transgenesis. The *Kuz-GFP*, *GFP-Tsp3A*, and *GFP-Tsp86D* BACs were inserted at the M{3xP3-RFP.attP′}ZH-51C, PBac{y[+]-attP-9A}VK00019 and PBac{y^{+}-attP-3B}VK00002 sites (Venken et al., 2006; Bischof et al., 2007). Transgenesis was performed by BestGene, Inc.

The *shmiR-Tsp3A* construct was designed according to Thermo Fisher Scientific software prediction (http://www.dharmacon.com/DesignCenter). Two positions (+715 and +792) were selected on the *Tsp3A* cDNA (GenBank/EMBL/DDBJ accession no. NM_080315). shmiR-*tsp3A*-1 (CGACCTGCAGAACTTCATTGA) and shmiR-*Tsp3A*-2 (GGAGCAAAAACGAGTACTTCA) knockdown oligonucleotides were modified to mimic the native *D. melanogaster* premiR-1 structure. The resultant *shmiR-Tsp3A* construct had mismatched bases at positions +2 and +11 as described in Haley et al. (2008). The shmiR-*Tsp3A*-1 (CTAGCAGTCGACCTGCAGTACTTCATTCATAGTTATATTCAAGCATATCAATGAAGTTCTGCAGGTCGGCG) and shmiR-*Tsp3A*-2 (CTAGCAGTGGAGCAAAAAGGAGTACTTGATAGTTATATTCAAGCATATGAAGTACTCGTTTTTGCTCCGCG) oligonucleotides were inserted into the HindIII–BamHI cloning sites of pHB (Haley et al., 2008). The resulting plasmids were used to generate transgenic flies using P-element transformation (BestGene, Inc.). The M[3xP3-RFP, NRE-pGR]86Fb was provided by S. Bray (University of Cambridge, Cambridge, England, UK; Housden et al., 2012). A detailed description of all genotypes is provided in Table S1.

Online supplemental material

Fig. S1 shows that TspanC8 tetraspanins represent an evolutionary conserved subfamily of tetraspanins. Fig. S2 shows genetic tools used in *Drosophila* studies. Fig. S3 shows functional redundancy between *Drosophila Tsp86D*, *Tsp26A*, and *Tsp3A*. Fig. S4 shows the effect of TspanC8 tetraspanins on ADAM17 surface expression and codistribution of Tspan10 and Tspan17 with CD63. Fig. S5 shows efficient and specific silencing of Tsp3A and Tsp86D in border cells. Table S1 provides a description of *Drosophila* genotypes.

We thank H. Bellen, S. Bray, C. Brou, R. Chance, J. Fischer, B. Haley, K. Irvine, T. Lieber, M. Martin-Bermudo, C. Rabouille, C. Saleh, P. Therond, M. Young, and the Bloomington Drosophila Stock Center, the Drosophila Genomics Resource Center, and Flybase for cells, antibodies, DNA, flies and other resources. Special thanks to R. Ueda and the National Institute of Genetics (Mishima, Japan), who kindly made available to us a collection of UAS-dsRNA transgenic lines. The 7G10, 2B10, 7E8A10 C458.2H, and C594.9B mAbs developed by G.M. Rubin, C. Goodman, and S. Artavanis-Tsakonas were obtained from the Developmental Studies Hybridoma Bank developed under the auspices of the NICHD and maintained by the University of Iowa, Department of Biology, Iowa City, IA 52242. We thank S. Leullier, L. Couturier, and the *Drosophila* RNAi Screening Platform for screening. We thank D. Clay for expert assistance in cell sorting and J. Chaker and M. Reyngoud for technical assistance. We are very grateful to R. Le Borgne for scientific discussions. We thank F. Bernard and all members of our laboratories for discussions and critical reading.

This work was funded by core funding from the INSERM, CNRS, and Institut Pasteur as well as by specific grants from the Association pour la Recherche sur le Cancer (to E. Rubinstein), NRB-Vaincre le Cancer (to E. Rubinstein), Institut du Cancer et d'Immunogénétique (to E. Rubinstein), Agence Nationale de la Recherche (05-BLAN-277 to F. Schweisguth), and Fondation pour la Recherche Médicale (DEQ20100318284 to F. Schweisguth). E. Dornier and J.-F. Ottavi were recipients of fellowships from the French ministry of Research. E. Dornier also received a fellowship from the Association pour la Recherche sur le Cancer and J.F. Ottavi from NRB-Vaincre le Cancer.

Submitted: 24 January 2012
Accepted: 27 September 2012

References

Arduise, C., T. Abache, L. Li, M. Billard, A. Chabanon, A. Ludwig, P. Mauduit, C. Boucheix, E. Rubinstein, and F. Le Naour. 2008. Tetraspanins regulate ADAM10-mediated cleavage of TNF-alpha and epidermal growth factor. *J. Immunol.* 181:7002–7013.

Berditchevski, F., E. Odintsova, S. Sawada, and E. Gilbert. 2002. Expression of the palmitoylation-deficient CD151 weakens the association of alpha 3 beta 1 integrin with the tetraspanin-enriched microdomains and affects integrin-dependent signaling. *J. Biol. Chem.* 277:36991–37000. http://dx.doi.org/10.1074/jbc.M205265200

Bischof, J., R.K. Maeda, M. Hediger, F. Karch, and K. Basler. 2007. An optimized transgenesis system for *Drosophila* using germ-line-specific

phiC31 integrases. *Proc. Natl. Acad. Sci. USA*. 104:3312–3317. http://dx.doi.org/10.1073/pnas.0611511104

Blobel, C.P. 2005. ADAMs: key components in EGFR signalling and development. *Nat. Rev. Mol. Cell Biol.* 6:32–43. http://dx.doi.org/10.1038/nrm1548

Boucheix, C., and E. Rubinstein. 2001. Tetraspanins. *Cell. Mol. Life Sci.* 58:1189–1205. http://dx.doi.org/10.1007/PL00000933

Bozkulak, E.C., and G. Weinmaster. 2009. Selective use of ADAM10 and ADAM17 in activation of Notch1 signaling. *Mol. Cell. Biol.* 29:5679–5695. http://dx.doi.org/10.1128/MCB.00406-09

Brou, C., F. Logeat, N. Gupta, C. Bessia, O. LeBail, J.R. Doedens, A. Cumano, P. Roux, R.A. Black, and A. Israël. 2000. A novel proteolytic cleavage involved in Notch signaling: the role of the disintegrin-metalloprotease TACE. *Mol. Cell*. 5:207–216. http://dx.doi.org/10.1016/S1097-2765(00)80417-7

Charrin, S., F. Le Naour, M. Oualid, M. Billard, G. Faure, S.M. Hanash, C. Boucheix, and E. Rubinstein. 2001. The major CD9 and CD81 molecular partner. Identification and characterization of the complexes. *J. Biol. Chem.* 276:14329–14337.

Charrin, S., S. Manié, M. Oualid, M. Billard, C. Boucheix, and E. Rubinstein. 2002. Differential stability of tetraspanin/tetraspanin interactions: role of palmitoylation. *FEBS Lett.* 516:139–144. http://dx.doi.org/10.1016/S0014-5793(02)02522-X

Charrin, S., F. Le Naour, V. Labas, M. Billard, J.P. Le Caer, J.F. Emile, M.A. Petit, C. Boucheix, and E. Rubinstein. 2003. EWI-2 is a new component of the tetraspanin web in hepatocytes and lymphoid cells. *Biochem. J.* 373:409–421. http://dx.doi.org/10.1042/BJ20030343

Charrin, S., F. le Naour, O. Silvie, P.E. Milhiet, C. Boucheix, and E. Rubinstein. 2009. Lateral organization of membrane proteins: tetraspanins spin their web. *Biochem. J.* 420:133–154. http://dx.doi.org/10.1042/BJ20082422

De Strooper, B., W. Annaert, P. Cupers, P. Saftig, K. Craessaerts, J.S. Mumm, E.H. Schroeter, V. Schrijvers, M.S. Wolfe, W.J. Ray, et al. 1999. A presenilin-1-dependent gamma-secretase-like protease mediates release of Notch intracellular domain. *Nature*. 398:518–522. http://dx.doi.org/10.1038/19083

del Álamo, D., H. Rouault, and F. Schweisguth. 2011. Mechanism and significance of cis-inhibition in Notch signalling. *Curr. Biol.* 21:R40–R47. http://dx.doi.org/10.1016/j.cub.2010.10.034

Dietzl, G., D. Chen, F. Schnorrer, K.C. Su, Y. Barinova, M. Fellner, B. Gasser, K. Kinsey, S. Oppel, S. Scheiblauer, et al. 2007. A genome-wide transgenic RNAi library for conditional gene inactivation in *Drosophila*. *Nature*. 448:151–156. http://dx.doi.org/10.1038/nature05954

Dunn, C.D., M.L. Sulis, A.A. Ferrando, and I. Greenwald. 2010. A conserved tetraspanin subfamily promotes Notch signaling in *Caenorhabditis elegans* and in human cells. *Proc. Natl. Acad. Sci. USA*. 107:5907–5912. http://dx.doi.org/10.1073/pnas.1001647107

Friggi-Grelin, F., C. Rabouille, and P. Therond. 2006. The cis-Golgi *Drosophila* GMAP has a role in anterograde transport and Golgi organization in vivo, similar to its mammalian ortholog in tissue culture cells. *Eur. J. Cell Biol.* 85:1155–1166. http://dx.doi.org/10.1016/j.ejcb.2006.07.001

Gho, M., M. Lecourtois, G. Géraud, J.W. Posakony, and F. Schweisguth. 1996. Subcellular localization of Suppressor of Hairless in *Drosophila* sense organ cells during Notch signalling. *Development*. 122:1673–1682.

Gordon, W.R., D. Vardar-Ulu, G. Histen, C. Sanchez-Irizarry, J.C. Aster, and S.C. Blacklow. 2007. Structural basis for autoinhibition of Notch. *Nat. Struct. Mol. Biol.* 14:295–300. http://dx.doi.org/10.1038/nsmb1227

Haley, B., D. Hendrix, V. Trang, and M. Levine. 2008. A simplified miRNA-based gene silencing method for *Drosophila melanogaster*. *Dev. Biol.* 321:482–490. http://dx.doi.org/10.1016/j.ydbio.2008.06.015

Hartenstein, V., and J.W. Posakony. 1990. A dual function of the Notch gene in *Drosophila* sensillum development. *Dev. Biol.* 142:13–30. http://dx.doi.org/10.1016/0012-1606(90)90147-B

Hartmann, D., B. de Strooper, L. Serneels, K. Craessaerts, A. Herreman, W. Annaert, L. Umans, T. Lübke, A. Lena Illert, K. von Figura, and P. Saftig. 2002. The disintegrin/metalloprotease ADAM 10 is essential for Notch signalling but not for alpha-secretase activity in fibroblasts. *Hum. Mol. Genet.* 11:2615–2624. http://dx.doi.org/10.1093/hmg/11.21.2615

He, Z.Y., S. Gupta, D. Myles, and P. Primakoff. 2009. Loss of surface EWI-2 on CD9 null oocytes. *Mol. Reprod. Dev.* 76:629–636. http://dx.doi.org/10.1002/mrd.20991

Heikens, M.J., T.M. Cao, C. Morita, S.L. Dehart, and S. Tsai. 2007. Penumbra encodes a novel tetraspanin that is highly expressed in erythroid progenitors and promotes effective erythropoiesis. *Blood*. 109:3244–3252. http://dx.doi.org/10.1182/blood-2006-09-046672

Heitzler, P., and P. Simpson. 1991. The choice of cell fate in the epidermis of *Drosophila*. *Cell*. 64:1083–1092. http://dx.doi.org/10.1016/0092-8674(91)90263-X

Hemler, M.E. 2005. Tetraspanin functions and associated microdomains. *Nat. Rev. Mol. Cell Biol.* 6:801–811. http://dx.doi.org/10.1038/nrm1736

Housden, B.E., K. Millen, and S.J. Bray. 2012. *Drosophila* reporter vectors compatible with PhiC31 integrase transgenesis techniques and their use to generate new Notch reporter fly lines. *G3 (Bethesda)*. 2:79–82.

Huang, S., S. Yuan, M. Dong, J. Su, C. Yu, Y. Shen, X. Xie, Y. Yu, X. Yu, S. Chen, et al. 2005. The phylogenetic analysis of tetraspanins projects the evolution of cell-cell interactions from unicellular to multicellular organisms. *Genomics*. 86:674–684. http://dx.doi.org/10.1016/j.ygeno.2005.08.004

Ivan, V., G. de Voer, D. Xanthakis, K.M. Spoorendonk, V. Kondylis, and C. Rabouille. 2008. *Drosophila* Sec16 mediates the biogenesis of tER sites upstream of Sar1 through an arginine-rich motif. *Mol. Biol. Cell*. 19:4352–4365. http://dx.doi.org/10.1091/mbc.E08-03-0246

Jarriault, S., C. Brou, F. Logeat, E.H. Schroeter, R. Kopan, and A. Israel. 1995. Signalling downstream of activated mammalian Notch. *Nature*. 377:355–358. http://dx.doi.org/10.1038/377355a0

Klein, T. 2002. kuzbanian is required cell autonomously during Notch signalling in the *Drosophila* wing. *Dev. Genes Evol.* 212:251–255. http://dx.doi.org/10.1007/s00427-002-0233-4

Kopan, R., and M.X. Ilagan. 2009. The canonical Notch signaling pathway: unfolding the activation mechanism. *Cell*. 137:216–233. http://dx.doi.org/10.1016/j.cell.2009.03.045

Lammich, S., E. Kojro, R. Postina, S. Gilbert, R. Pfeiffer, M. Jasionowski, C. Haass, and F. Fahrenholz. 1999. Constitutive and regulated alpha-secretase cleavage of Alzheimer's amyloid precursor protein by a disintegrin metalloprotease. *Proc. Natl. Acad. Sci. USA*. 96:3922–3927. http://dx.doi.org/10.1073/pnas.96.7.3922

Lecourtois, M., and F. Schweisguth. 1998. Indirect evidence for Delta-dependent intracellular processing of notch in *Drosophila* embryos. *Curr. Biol.* 8:771–774. http://dx.doi.org/10.1016/S0960-9822(98)70300-8

Lee, J.H., E. Overstreet, E. Fitch, S. Fleenor, and J.A. Fischer. 2009. *Drosophila* liquid facets-Related encodes Golgi epsin and is an essential gene required for cell proliferation, growth, and patterning. *Dev. Biol.* 331:1–13. http://dx.doi.org/10.1016/j.ydbio.2009.03.029

Lieber, T., S. Kidd, and M.W. Young. 2002. kuzbanian-mediated cleavage of *Drosophila* Notch. *Genes Dev.* 16:209–221. http://dx.doi.org/10.1101/gad.942302

Manseau, L., A. Baradaran, D. Brower, A. Budhu, F. Elefant, H. Phan, A.V. Philp, M. Yang, D. Glover, K. Kaiser, et al. 1997. GAL4 enhancer traps expressed in the embryo, larval brain, imaginal discs, and ovary of *Drosophila*. *Dev. Dyn.* 209:310–322. http://dx.doi.org/10.1002/(SICI)1097-0177(199707)209:3<310::AID-AJA6>3.0.CO;2-L

Marcello, E., F. Gardoni, M. Di Luca, and I. Pérez-Otaño. 2010. An arginine stretch limits ADAM10 exit from the endoplasmic reticulum. *J. Biol. Chem.* 285:10376–10384. http://dx.doi.org/10.1074/jbc.M109.055947

Meloty-Kapella, L., B. Shergill, J. Kuon, E. Botvinick, and G. Weinmaster. 2012. Notch ligand endocytosis generates mechanical pulling force dependent on dynamin, epsins, and actin. *Dev. Cell*. 22:1299–1312. http://dx.doi.org/10.1016/j.devcel.2012.04.005

Michelsen, K., H. Yuan, and B. Schwappach. 2005. Hide and run. Arginine-based endoplasmic-reticulum-sorting motifs in the assembly of heteromultimeric membrane proteins. *EMBO Rep.* 6:717–722. http://dx.doi.org/10.1038/sj.embor.7400480

Mishra-Gorur, K., M.D. Rand, B. Perez-Villamil, and S. Artavanis-Tsakonas. 2002. Down-regulation of Delta by proteolytic processing. *J. Cell Biol.* 159:313–324. http://dx.doi.org/10.1083/jcb.200203117

Moretti, J., P. Chastagner, S. Gastaldello, S.F. Heuss, A.M. Dirac, R. Bernards, M.G. Masucci, A. Israël, and C. Brou. 2010. The translation initiation factor 3f (eIF3f) exhibits a deubiquitinase activity regulating Notch activation. *PLoS Biol.* 8:e1000545. http://dx.doi.org/10.1371/journal.pbio.1000545

Mumm, J.S., E.H. Schroeter, M.T. Saxena, A. Griesemer, X. Tian, D.J. Pan, W.J. Ray, and R. Kopan. 2000. A ligand-induced extracellular cleavage regulates gamma-secretase-like proteolytic activation of Notch1. *Mol. Cell*. 5:197–206. http://dx.doi.org/10.1016/S1097-2765(00)80416-5

Mummery-Widmer, J.L., M. Yamazaki, T. Stoeger, M. Novatchkova, S. Bhalerao, D. Chen, G. Dietzl, B.J. Dickson, and J.A. Knoblich. 2009. Genome-wide analysis of Notch signalling in *Drosophila* by transgenic RNAi. *Nature*. 458:987–992. http://dx.doi.org/10.1038/nature07936

Nolo, R., L.A. Abbott, and H.J. Bellen. 2000. Senseless, a Zn finger transcription factor, is necessary and sufficient for sensory organ development in *Drosophila*. *Cell*. 102:349–362. http://dx.doi.org/10.1016/S0092-8674(00)00040-4

Okajima, T., A. Xu, L. Lei, and K.D. Irvine. 2005. Chaperone activity of protein O-fucosyltransferase 1 promotes notch receptor folding. *Science*. 307:1599–1603. http://dx.doi.org/10.1126/science.1108995

Pan, D., and G.M. Rubin. 1997. Kuzbanian controls proteolytic processing of Notch and mediates lateral inhibition during *Drosophila* and vertebrate neurogenesis. *Cell*. 90:271–280. http://dx.doi.org/10.1016/S0092-8674(00)80335-9

Parks, A.L., K.R. Cook, M. Belvin, N.A. Dompe, R. Fawcett, K. Huppert, L.R. Tan, C.G. Winter, K.P. Bogart, J.E. Deal, et al. 2004. Systematic generation of high-resolution deletion coverage of the *Drosophila melanogaster* genome. *Nat. Genet.* 36:288–292. http://dx.doi.org/10.1038/ng1312

Prox, J., M. Willenbrock, S. Weber, T. Lehmann, D. Schmidt-Arras, R. Schwanbeck, P. Saftig, and M. Schwake. 2012. Tetraspanin15 regulates cellular trafficking and activity of the ectodomain sheddase ADAM10. *Cell. Mol. Life Sci.* 69:2919–2932. http://dx.doi.org/10.1007/s00018-012-0960-2

Qi, H., M.D. Rand, X. Wu, N. Sestan, W. Wang, P. Rakic, T. Xu, and S. Artavanis-Tsakonas. 1999. Processing of the notch ligand delta by the metalloprotease Kuzbanian. *Science*. 283:91–94. http://dx.doi.org/10.1126/science.283.5398.91

Reiss, K., and P. Saftig. 2009. The "a disintegrin and metalloprotease" (ADAM) family of sheddases: physiological and cellular functions. *Semin. Cell Dev. Biol.* 20:126–137. http://dx.doi.org/10.1016/j.semcdb.2008.11.002

Rørth, P., K. Szabo, A. Bailey, T. Laverty, J. Rehm, G.M. Rubin, K. Weigmann, M. Milán, V. Benes, W. Ansorge, and S.M. Cohen. 1998. Systematic gain-of-function genetics in *Drosophila*. *Development*. 125:1049–1057.

Saftig, P., and K. Reiss. 2011. The "A Disintegrin And Metalloproteases" ADAM10 and ADAM17: novel drug targets with therapeutic potential? *Eur. J. Cell Biol.* 90:527–535. http://dx.doi.org/10.1016/j.ejcb.2010.11.005

Schroeter, E.H., J.A. Kisslinger, and R. Kopan. 1998. Notch-1 signalling requires ligand-induced proteolytic release of intracellular domain. *Nature*. 393:382–386. http://dx.doi.org/10.1038/30756

Serru, V., F. Le Naour, M. Billard, D.O. Azorsa, F. Lanza, C. Boucheix, and E. Rubinstein. 1999. Selective tetraspan-integrin complexes (CD81/α4β1, CD151/α3β1, CD151/α6β1) under conditions disrupting tetraspan interactions. *Biochem. J.* 340:103–111. http://dx.doi.org/10.1042/0264-6021:3400103

Serru, V., P. Dessen, C. Boucheix, and E. Rubinstein. 2000. Sequence and expression of seven new tetraspans. *Biochim. Biophys. Acta*. 1478:159–163. http://dx.doi.org/10.1016/S0167-4838(00)00022-4

Shoham, T., R. Rajapaksa, C. Boucheix, E. Rubinstein, J.C. Poe, T.F. Tedder, and S. Levy. 2003. The tetraspanin CD81 regulates the expression of CD19 during B cell development in a postendoplasmic reticulum compartment. *J. Immunol.* 171:4062–4072.

Six, E.M., D. Ndiaye, G. Sauer, Y. Laâbi, R. Athman, A. Cumano, C. Brou, A. Israël, and F. Logeat. 2004. The notch ligand Delta1 recruits Dlg1 at cell-cell contacts and regulates cell migration. *J. Biol. Chem.* 279:55818–55826. http://dx.doi.org/10.1074/jbc.M408022200

Sotillos, S., F. Roch, and S. Campuzano. 1997. The metalloprotease-disintegrin Kuzbanian participates in Notch activation during growth and patterning of *Drosophila* imaginal discs. *Development*. 124:4769–4779.

Spandidos, A., X. Wang, H. Wang, and B. Seed. 2010. PrimerBank: a resource of human and mouse PCR primer pairs for gene expression detection and quantification. *Nucleic Acids Res.* 38(Database issue):D792–D799. http://dx.doi.org/10.1093/nar/gkp1005

Stipp, C.S., T.V. Kolesnikova, and M.E. Hemler. 2001a. EWI-2 is a major CD9 and CD81 partner and member of a novel Ig protein subfamily. *J. Biol. Chem.* 276:40545–40554. http://dx.doi.org/10.1074/jbc.M107338200

Stipp, C.S., D. Orlicky, and M.E. Hemler. 2001b. FPRP, a major, highly stoichiometric, highly specific CD81- and CD9-associated protein. *J. Biol. Chem.* 276:4853–4862. http://dx.doi.org/10.1074/jbc.M009859200

Stipp, C.S., T.V. Kolesnikova, and M.E. Hemler. 2003. EWI-2 regulates alpha3beta1 integrin-dependent cell functions on laminin-5. *J. Cell Biol.* 163:1167–1177. http://dx.doi.org/10.1083/jcb.200309113

Struhl, G., and A. Adachi. 1998. Nuclear access and action of notch in vivo. *Cell*. 93:649–660. http://dx.doi.org/10.1016/S0092-8674(00)81193-9

Tiyanont, K., T.E. Wales, M. Aste-Amezaga, J.C. Aster, J.R. Engen, and S.C. Blacklow. 2011. Evidence for increased exposure of the Notch1 metalloprotease cleavage site upon conversion to an activated conformation. *Structure*. 19:546–554. http://dx.doi.org/10.1016/j.str.2011.01.016

van Tetering, G., P. van Diest, I. Verlaan, E. van der Wall, R. Kopan, and M. Vooijs. 2009. Metalloprotease ADAM10 is required for Notch1 site 2 cleavage. *J. Biol. Chem.* 284:31018–31027. http://dx.doi.org/10.1074/jbc.M109.006775

Venken, K.J., Y. He, R.A. Hoskins, and H.J. Bellen. 2006. P[acman]: a BAC transgenic platform for targeted insertion of large DNA fragments in D. *melanogaster*. *Science*. 314:1747–1751. http://dx.doi.org/10.1126/science.1134426

Venken, K.J., J.W. Carlson, K.L. Schulze, H. Pan, Y. He, R. Spokony, K.H. Wan, M. Koriabine, P.J. de Jong, K.P. White, et al. 2009. Versatile P[acman] BAC libraries for transgenesis studies in *Drosophila melanogaster*. *Nat. Methods*. 6:431–434. http://dx.doi.org/10.1038/nmeth.1331

Wakabayashi, T., K. Craessaerts, L. Bammens, M. Bentahir, F. Borgions, P. Herdewijn, A. Staes, E. Timmerman, J. Vandekerckhove, E. Rubinstein, et al. 2009. Analysis of the gamma-secretase interactome and validation of its association with tetraspanin-enriched microdomains. *Nat. Cell Biol.* 11:1340–1346. http://dx.doi.org/10.1038/ncb1978

Wang, X., J. Bo, T. Bridges, K.D. Dugan, T.C. Pan, L.A. Chodosh, and D.J. Montell. 2006. Analysis of cell migration using whole-genome expression profiling of migratory cells in the *Drosophila* ovary. *Dev. Cell*. 10:483–495. http://dx.doi.org/10.1016/j.devcel.2006.02.003

Wang, X., J.C. Adam, and D. Montell. 2007. Spatially localized Kuzbanian required for specific activation of Notch during border cell migration. *Dev. Biol.* 301:532–540. http://dx.doi.org/10.1016/j.ydbio.2006.08.031

Wen, C., M.M. Metzstein, and I. Greenwald. 1997. SUP-17, a *Caenorhabditis elegans* ADAM protein related to *Drosophila* KUZBANIAN, and its role in LIN-12/NOTCH signalling. *Development*. 124:4759–4767.

Wu, C., C. Orozco, J. Boyer, M. Leglise, J. Goodale, S. Batalov, C.L. Hodge, J. Haase, J. Janes, J.W. Huss III, and A.I. Su. 2009. BioGPS: an extensible and customizable portal for querying and organizing gene annotation resources. *Genome Biol.* 10:R130. http://dx.doi.org/10.1186/gb-2009-10-11-r130

Xu, D., C. Sharma, and M.E. Hemler. 2009. Tetraspanin12 regulates ADAM10-dependent cleavage of amyloid precursor protein. *FASEB J.* 23:3674–3681. http://dx.doi.org/10.1096/fj.09-133462

Yang, X., C. Claas, S.K. Kraeft, L.B. Chen, Z. Wang, J.A. Kreidberg, and M.E. Hemler. 2002. Palmitoylation of tetraspanin proteins: modulation of CD151 lateral interactions, subcellular distribution, and integrin-dependent cell morphology. *Mol. Biol. Cell*. 13:767–781. http://dx.doi.org/10.1091/mbc.01-05-0275

Yauch, R.L., F. Berditchevski, M.B. Harler, J. Reichner, and M.E. Hemler. 1998. Highly stoichiometric, stable, and specific association of integrin alpha3beta1 with CD151 provides a major link to phosphatidylinositol 4-kinase, and may regulate cell migration. *Mol. Biol. Cell*. 9:2751–2765.

Published October 22, 2012

Dornier et al., http://www.jcb.org/cgi/content/full/jcb.201201133/DC1

A

	Tspan5	Tspan17	Tspan14	Tsp26A	Tsp12	Tspan33	Tsp86D	Tsp3A	Tspan15	Tspan10	CD151
Tspan5	100	64	56	44	38	37	35	33	28	25	22
Tspan17			46	36	30	33	31	30	24	24	20
Tspan14				40	32	34	35	33	27	24	22
Tsp26A					36	28	30	31	25	22	23
Tsp12						27	28	30	21	22	19
Tspan33							37	35	28	25	21
Tsp86D								74	25	27	22
Tsp3A									25	25	21
Tspan15										19	19
Tspan10											18
CD151											100

B

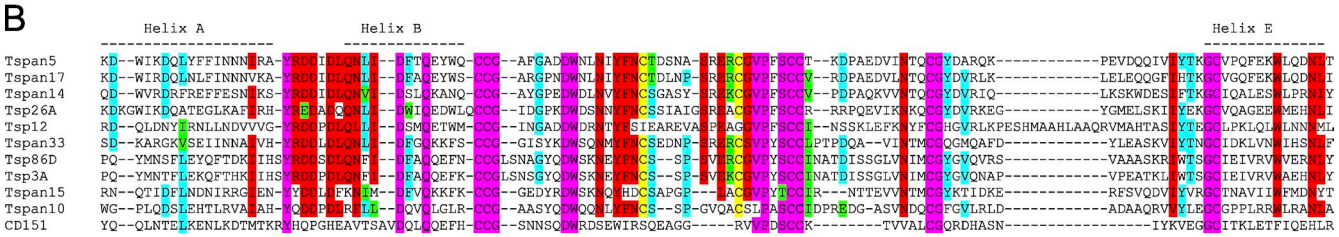

Figure S1. **An evolutionary conserved subfamily of tetraspanins.** (A) Amino acid identity levels between *H. sapiens* (Tspan5, 17, 14, 33, 15, 10), *D. melanogaster* (Tsp26A, 86D, 3A), and *C. elegans* (Tsp12) TspanC8 tetraspanins. The prototypal tetraspanin CD151 is also included for comparison. Human tetraspanins have most often less than 30% identity with each other. (B) Sequence alignment of the second extracellular domain of CD151 and the different *H. sapiens*, *D. melanogaster*, and *C. elegans* TspanC8 tetraspanins. This domain is highly divergent within the tetraspanin superfamily with the exception of a few residues that probably maintain the tetraspanin fold (pink). In contrast, TspanC8 tetraspanins share many conserved residues (red, >80% conservation; blue, >60% conservation; green, conservative substitutions) within this domain. The two additional cysteines that are the hallmark of TspanC8 are in yellow. Note that although Tsp12 has only six cysteines in the large extracellular domain, it shares many residues characteristic of TspanC8. The three conserved helices of this domain are shown on top of the sequences.

Published October 22, 2012

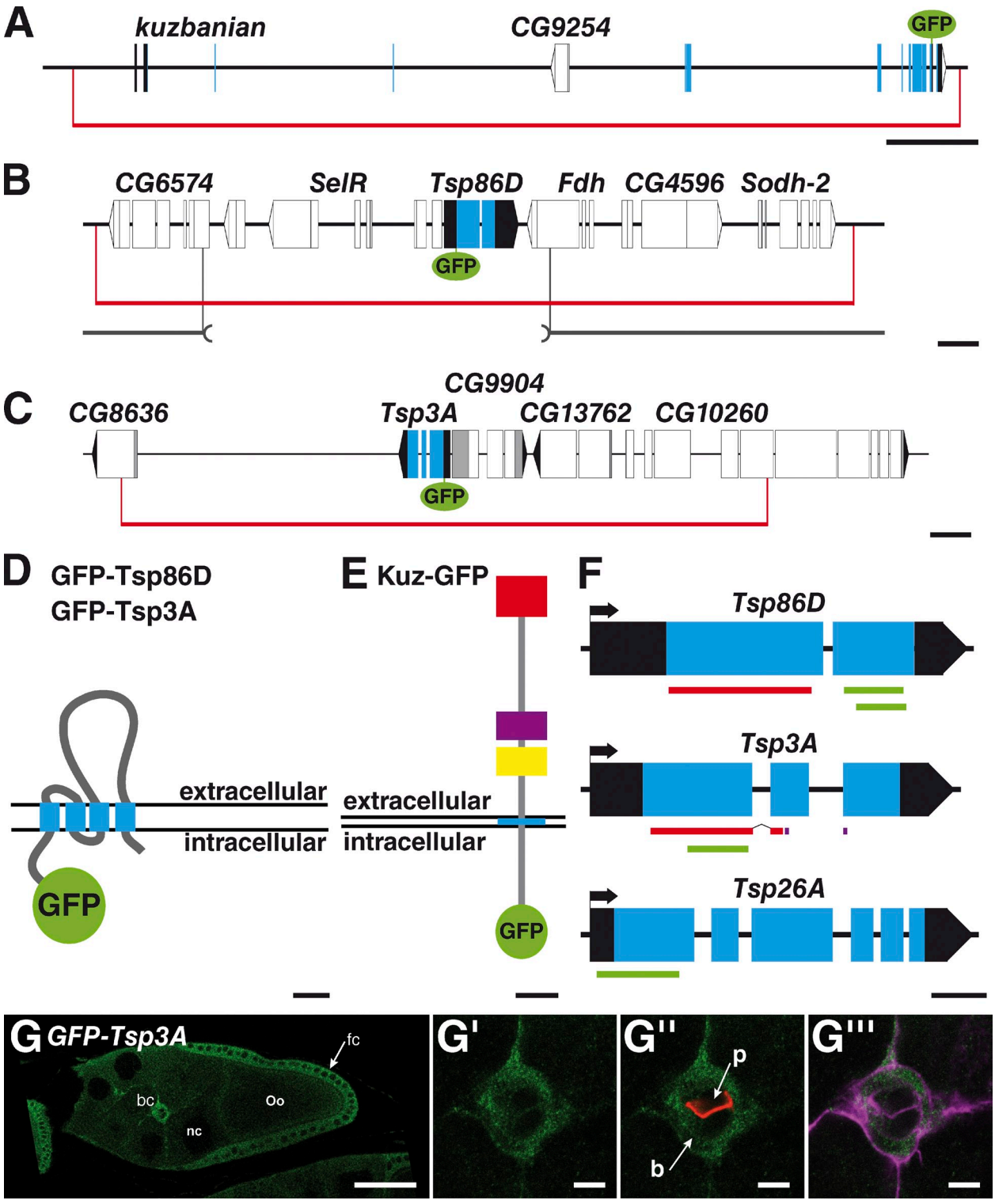

Figure S2. **Genetic tools.** (A–C) Schematic representation of the *kuz* (A), *Tsp86D* (B), and *Tsp3A* (C) genomic regions. The *kuz*, *Tsp86D*, and *Tsp3A* open reading frame (ORF) are in blue. 5′ and 3′ UTRs are in black. Exons from neighboring genes are in white. The BACs used in this study are indicated in red. GFP (green) was inserted at the 3′ and 5′ ends of *kuz* and *Tsp86D/Tsp3A* ORFs, respectively. The $Tsp86D^{\Delta 3}$ deficiency is indicated in gray. Bars: (A) 10 kb; (B and C) 1 kb. (D and E) Domain structure of GFP-Tsp86D/3A and Kuz-GFP (transmembrane segment, blue; prodomain of Kuz, red; metalloprotease domain, purple; disintegrin domain, yellow; GFP, green). Bars: (D) 20 aa; (E) 200 aa. (F) Sequence targeted by the dsRNAi and shmiR constructs used in this study (NIG-Fly, red; VDRC, green; shmiR, purple). The *Tsp86D*, *Tsp26A*, and *Tsp3A* transcripts are represented as in B. Bar, 200 nt. (G–G′′′) GFP-Tsp3A (anti-GFP, green; Fas3, red in G′′; actin, red in G′′′) was detected in migrating border cells (b) and in follicular cells. Polar cells (p) exhibited lower levels of GFP-Tsp3A. GFP-Tsp3A appears to be expressed similarly as GFP-Tsp86D and complementary to Kuz-GFP (see Fig. 6). Bars: (G) 40 µm; (G′and G′′) 5 µm.

Published October 22, 2012

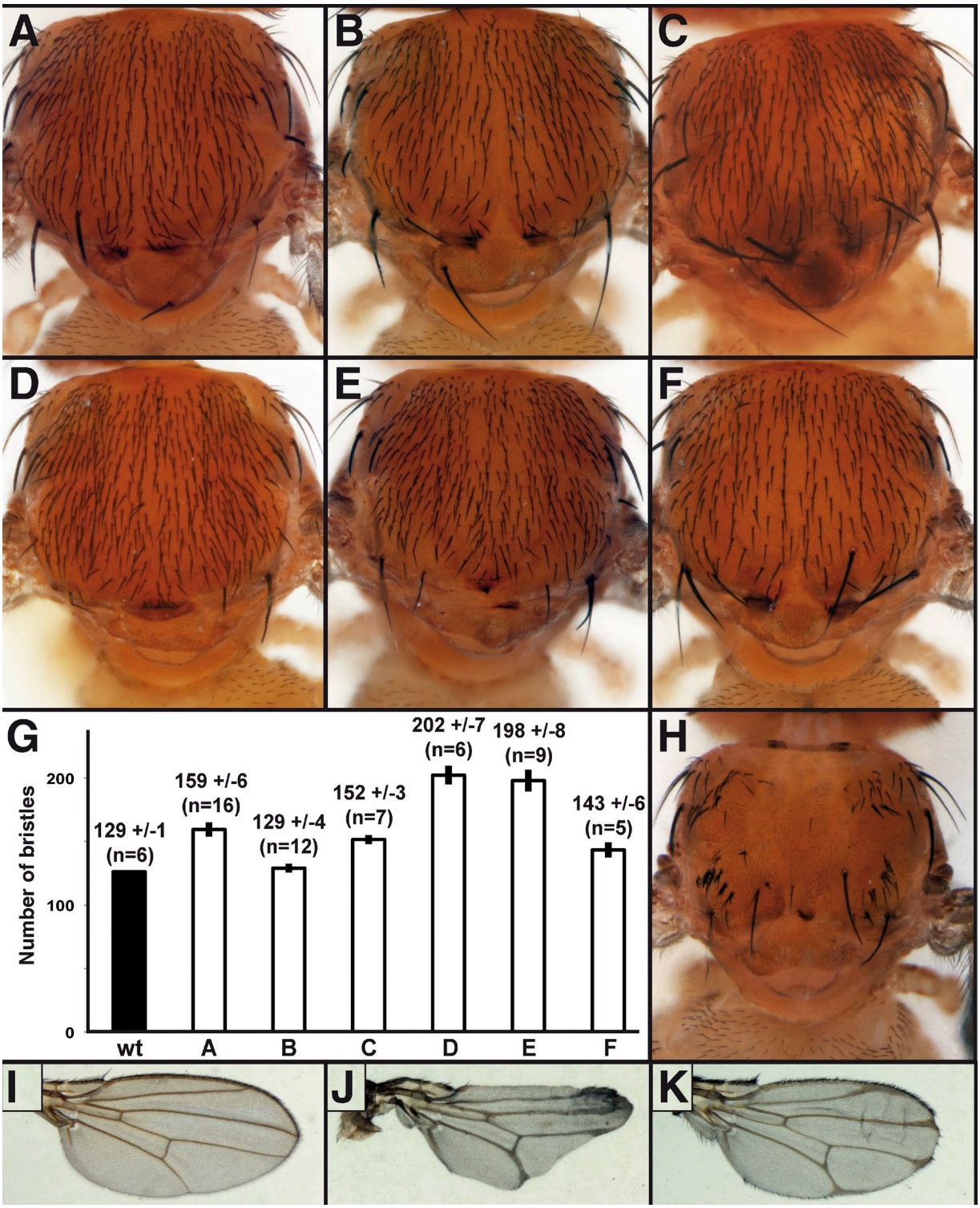

Figure S3. **Functional redundancy between *Drosophila Tsp86D, Tsp26A,* and *Tsp3A*.** (A–F) Pattern of sensory organs in adult flies silenced for *Tsp3A* (A), *Tsp26A* (B), *Tsp86D* (C), *Tsp3A* and *Tsp26A* (D), *Tsp3A* in a *Tsp86D* heterozygous background (E), and *Tsp26A* in a *Tsp86D* heterozygous background (F). Silencing was achieved using *ap*-GAL4. See Fig. 2 for a wild-type control and Table S1 for complete genotypes. (G) Histogram showing the number of bristles located in dorsal-central rows 1–5 of the notum (*n* is the number of scored flies for each genotype). The genotypes are indicated by letters corresponding to the other panels of this figure. For each genotype (except B), the distribution was significantly different from wild type (wt; χ^2 test, $P < 0.01$). (I–K) Wing margin and vein pattern in adult flies silenced for *kuz* (J) and *Tsp3A*, *Tsp26A*, and *Tsp86D* (K). Silencing was performed using *sd*-GAL4. A wild-type control is shown in I. Loss of TspanC8 activity in the wing results in wing nicks and vein-thickening *Notch*-like phenotypes that are milder than those seen upon the silencing of *kuz*.

Published October 22, 2012

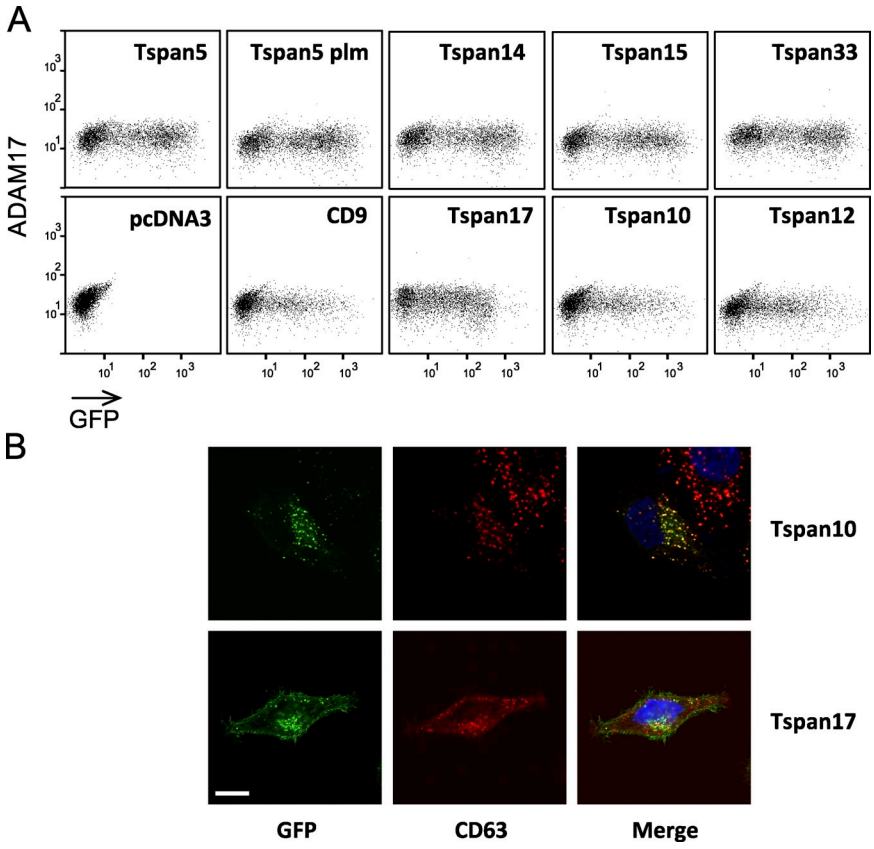

Figure S4. **Effect of TspanC8 tetraspanins on ADAM17 surface expression and codistribution of Tspan10 and Tspan17 with CD63.** (A) Flow cytometry analysis of the surface expression of ADAM17 in HeLa cells transiently transfected with different GFP-tagged tetraspanins. (B) Confocal microscopy analysis of GFP-tagged Tspan10 and Tspan17 (green) and CD63 (red) localization (red) in permeabilized HeLa cells. Bar, 10 µm. These experiments were performed at least twice.

Published October 22, 2012

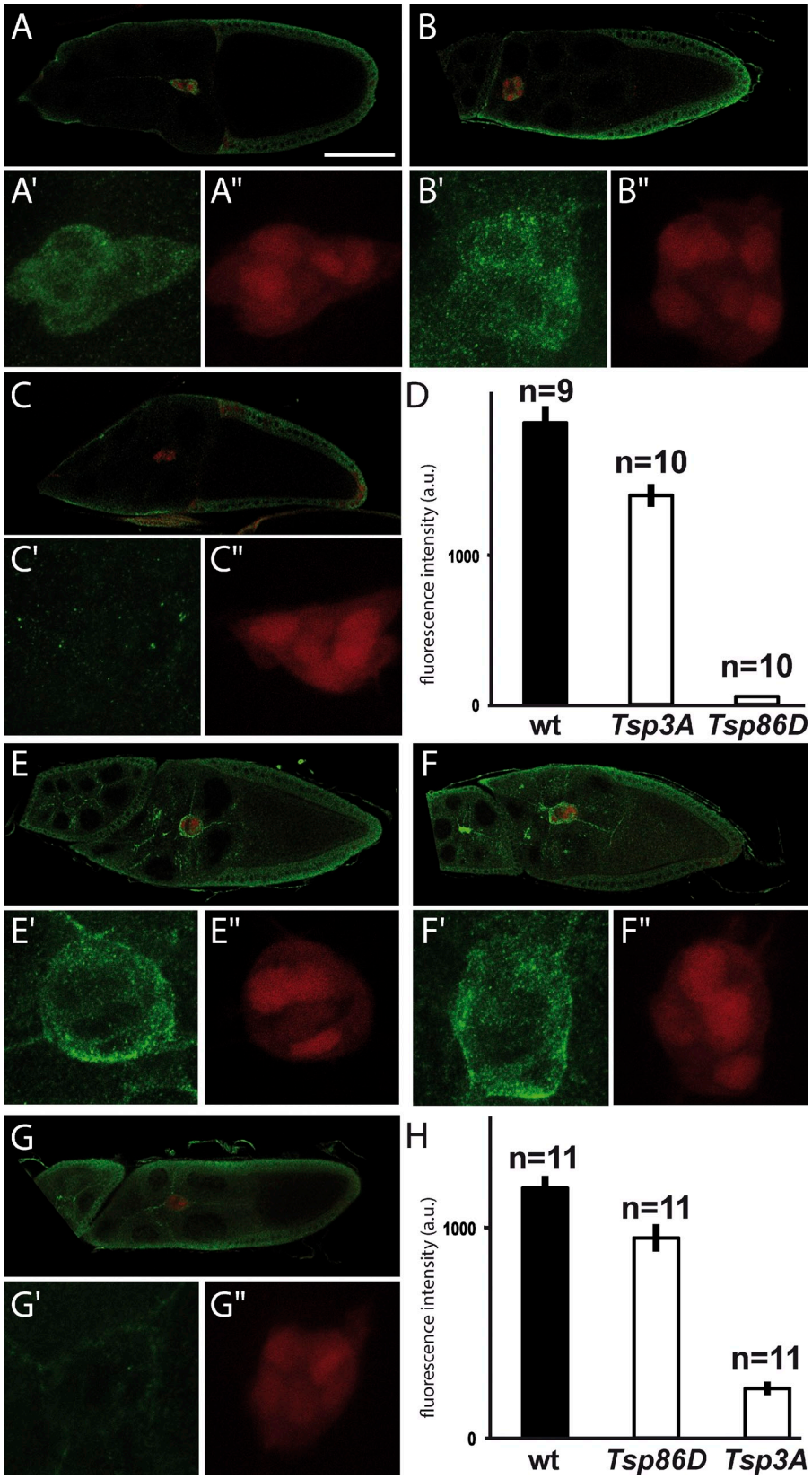

Figure S5. **Efficient and specific silencing of Tsp3A and Tsp86D in border cells.** (A–D) The expression of GFP-Tsp86D (green) was efficiently and specifically silenced in border cells (marked by the expression of RFP under the control of *slbo*-GAL4) by dsRNA directed against Tsp86D (C–C′′). In the absence of dsRNA (A–A′′) or in the presence of dsRNA directed against Tsp3A (B–B′′), GFP-Tsp86D was detected in border cells. The GFP fluorescence signal was measured to estimate the relative levels of GFP-Tsp86D (D; a.u.: arbitrary units). (E–G′′) Conversely, the expression of GFP-Tsp3A (green; no dsRNA in E–E′′) was efficiently silenced by dsRNA directed against Tsp3A (G–G′′) expressed but not by Tsp86D dsRNA (F–F′′). Unfortunately, the expression of GFP-Tsp3A and GFP-Tsp86D was too low in imaginal tissues to evaluate the efficiency of silencing in these tissues. (H) Quantification of the GFP-Tsp3A signal as in D.

Published October 22, 2012

Table S1. **Genotypes**

Figures	Genotypes
Fig. 2, A–C	w; ap-GAL4/+
Fig. 2, D–F	w; ap-GAL4/UAS-dsRNA *tsp3A*, UAS-dsRNA *tsp26A*; *Tsp86D*$^{[\Delta 3]}$/+
Fig. 2, G and H	(Tsp3A^{RNAi}): y w P[ry, hs-FLP]1.22 P[mw, ptub-GAL4] P[mw, UAS-GFP]/w; UAS-dsRNA *tsp3A*/+; P[neo, FRT]82B, P[mw, ptub-GAL80]/P[ry, neo, FRT]82B
Fig. 2 H	(Tsp26A^{RNAi}): y w P[ry, hs-FLP]1.22 P[mw, ptub-GAL4] P[mw, UAS-GFP]/w; UAS-dsRNA *tsp26A*/+; P[neo,FRT]82B, P[mw, ptub-GAL80]/P[ry, neo, FRT]82B
Fig. 2 H	(Tsp86D^{RNAi}): y w P[ry, hs-FLP]1.22 P[mw, ptub-GAL4] P[mw, UAS-GFP]/w; P[neo, FRT]40A, P[mw, ptub-GAL80]/P[ry, neo, FRT]40A; UAS-dsRNA *tsp86D*/+
Fig. 2 H	(Tsp86D$^{[\Delta 3]}$): y w P[ry, hs-FLP]1.22 P[mw, ptub-GAL4] P[mw, UAS-GFP]/w; ; P[neo, FRT]82B, P[mw, ptub-GAL80]/P[ry, neo, FRT]82B, *Tsp86D*$^{[\Delta 3]}$
Fig. 2 H	(wt): y w P[ry, hs-FLP]1.22 P[mw, ptub-GAL4] P[mw, UAS-GFP]/w; ; P[neo, FRT]82B, P[mw, ptub-GAL80]/P[ry, neo, FRT]82B
Fig. 7, B, C, and H	(wt): w, c306-Gal4/w; slbo-GAL4, UAS-GFP/+
Fig. 7, B, C, and H	(TspanC8): w, c306-Gal4/w; slbo-GAL4, UAS-GFP/UAS-dsRNA *tsp3A*, UAS-dsRNA *tsp26A* ; UAS-dsRNA *tsp86D*/+
Fig. 7, B and C	(kuz): w, c306-Gal4/w; slbo-GAL4, UAS-GFP/dsRNA *kuz*
Fig. 7, D–D′′′	w; M[3xP3-RFP.attP.w+.*kuz*^{GFP}]51C/M[3xP3-RFP.attP.w+ *kuz*^{GFP}]51C
Fig. 7, E–E′′′	w; PBac{y[+]-attP-3B. ^{GFP}*tsp86D*}VK00002/PBac{y[+]-attP-3B. ^{GFP}*tsp86D*}VK00002
Fig. 7, F–F′ and L	(wt): w; slbo-GAL4, M[3xP3-RFP.attP.w+.*kuz*^{GFP}]51C/+
Fig. 7, G–G′ and L	(TspanC8): w; slbo-GAL4, M[3xP3-RFP.attP.w+.*kuz*^{GFP}]51C/UAS-dsRNA *tsp3A*, UAS-dsRNA *tsp26A*; UAS-dsRNA *tsp86D*/+
Fig. 7, I–I′ and L	(wt): w; slbo-Gal4/+; M[3xP3-RFP, NRE-pGR]86Fb/+
Fig. 7, J–J′, K–K′, and L	(TspanC8): w; slbo-Gal4/UAS-dsRNA *tsp3A*, UAS-dsRNA *tsp26A*; M[3xP3-RFP, NRE-pGR]86Fb/UAS-dsRNA *tsp86D*
Fig. 7 L	(kuz): w; slbo-Gal4/UAS-dsRNA *kuz*; M[3xP3-RFP, NRE-pGR]86Fb/+
Fig. S2, G–G′′′	w/w; PBac{y[+]-attP-9A. ^{GFP}*tsp3A* }VK00019/PBac{y[+]-attP-9A. ^{GFP}*tsp3A* }VK00019
Fig. S3 A	w/w; ap-GAL4/+; UAS-dsRNA *tsp3A*/+
Fig. S3 B	w/w; ap-GAL4/+; UAS-dsRNA *tsp86D*/+
Fig. S3 C	w/w; ap-GAL4/UAS-dsRNA *tsp26A*
Fig. S3 D	w/w; ap-GAL4/UAS-dsRNA *tsp3A*, UAS-dsRNA *tsp26A*
Fig. S3 E	w/w; ap-GAL4/UAS-dsRNA *tsp3A*; tsp86D$^{[\Delta 3]}$/+
Fig. S3 F	w/w; ap-GAL4/UAS-dsRNA *tsp26A*; tsp86D$^{[\Delta 3]}$/+
Fig. S3 H; Fig. 2, I–I′′ and J–J′′	w/w; ap-GAL4/UAS-dsRNA *tsp3A*, UAS-dsRNA *tsp26A*; UAS-dsRNA *tsp86D*/+
Fig. S3 I	w, sd-GAL4/w
Fig. S3 J	w, sd-GAL4/w; UAS-dsRNA *tsp3A*, UAS-dsRNA *tsp26A*/+; UAS-dsRNA *tsp86D*/+
Fig. S3 K	w, sd-GAL4/w; UAS-dsRNA *kuz*
Fig. S5, A–A′′ and D	(wt): w/w; slbo-Gal4, UAS-nlsRFP/PBac{y[+]-attP-3B. ^{GFP}*tsp86D*}VK00002
Fig. S5, B–B′′ and D	(Tsp3A): w/w; slbo-Gal4, UAS-nlsRFP/PBac{y[+]-attP-3B. ^{GFP}*tsp86D*}VK00002; UAS-dsRNA *tsp3A*/+
Fig. S5, C–C′′ and D	(Tsp86D): w/w; slbo-Gal4, UAS-nlsRFP/PBac{y[+]-attP-3B. ^{GFP}*tsp86D*}VK00002; UAS-dsRNA *tsp86D*/+
Fig. S5, E–E′ and H	(wt): w/w; slbo-Gal4, UAS-nlsRFP/CyO; PBac{y[+]-attP-9A. ^{GFP}*tsp3A* }VK00019/+
Fig. S5, F–F′′ and H	(Tsp86D): w/w; slbo-Gal4, UAS-nlsRFP/UAS-dsRNA *tsp86D*/+; PBac{y[+]-attP-9A. ^{GFP}*tsp3A* }VK00019/+
Fig. S5, G–G′′ and H	(Tsp3A): w/w; slbo-Gal4, UAS-nlsRFP/UAS-dsRNA *tsp3A*/+; PBac{y[+]-attP-9A. ^{GFP}*tsp3A* }VK00019/+